

# IMPROVED POWER-BASED LATERATION VIA WALL ATTENUATION FACTOR

Bachelorarbeit  
der Philosophisch-naturwissenschaftlichen Fakultät  
der Universität Bern

vorgelegt von

Urs Zysset  
11-122-165  
2015

Betreuer der Arbeit:  
Zan Li

Leiter der Arbeit:  
Professor Dr. Torsten Braun  
Institut für Informatik und angewandte Mathematik  
Research group Communication and Distributed Systems





# Contents

<b>Contents</b>	<b>i</b>
<b>List of Figures</b>	<b>iii</b>
<b>List of Tables</b>	<b>v</b>
<b>1 Introduction</b>	<b>1</b>
<b>2 Theoretical Background of Indoor Localization</b>	<b>3</b>
2.1 Signal Propagation . . . . .	3
2.2 Localization Algorithms . . . . .	4
2.2.1 Range Free Localization . . . . .	5
2.2.2 Range Based Localization . . . . .	6
<b>3 Developed Indoor Localization Algorithm</b>	<b>9</b>
3.1 Preparation . . . . .	10
3.2 Step 1: Proximity . . . . .	10
3.3 Step 2: Shadowing . . . . .	11
3.3.1 Wall Approximation . . . . .	11
3.3.2 Path Loss Model . . . . .	12
3.3.3 Threshold . . . . .	13
3.4 Step 3: Localization . . . . .	14
3.4.1 Linear Least Square . . . . .	15
3.4.2 Trilateration . . . . .	16
3.4.3 Adaptive Geometric Algorithm . . . . .	16
<b>4 Preliminary Experimental Analysis</b>	<b>19</b>
4.1 Practical Measurements . . . . .	19
4.1.1 Hardware . . . . .	19
4.1.2 Software . . . . .	19
4.1.3 Environment . . . . .	20
4.1.4 Site Survey . . . . .	20
4.1.5 Corridor Measurement . . . . .	20
4.2 Path Loss Model Derivation . . . . .	21

4.3	Proximity Algorithm . . . . .	22
4.4	Wall Attenuation . . . . .	25
4.5	Threshold . . . . .	26
<b>5</b>	<b>Evaluation of WAILA</b>	<b>29</b>
5.1	Evaluation Measurements . . . . .	29
5.2	Performance in the Static Measurement . . . . .	30
5.2.1	Weighted Centroid . . . . .	30
5.2.2	Wall Attenuation Indoor Localization Algorithm . . . . .	32
5.3	Performance in the Dynamic Measurement . . . . .	37
5.3.1	Weighted Centroid . . . . .	37
5.3.2	Wall Attenuation Indoor Localization Algorithm . . . . .	38
<b>6</b>	<b>Conclusions</b>	<b>43</b>
6.1	Summary & Conclusions . . . . .	43
6.2	Future Work . . . . .	43
	<b>Appendices</b>	<b>45</b>
<b>A</b>	<b>Site Survey</b>	<b>47</b>
<b>B</b>	<b>Corridor Path Loss Model</b>	<b>49</b>
<b>C</b>	<b>Static Measurement</b>	<b>51</b>
<b>D</b>	<b>Dynamic Measurement</b>	<b>53</b>
<b>E</b>	<b>Localization Errors</b>	<b>55</b>
	<b>List of Abbreviations</b>	<b>57</b>
	<b>Bibliography</b>	<b>59</b>

# List of Figures

3.1	Wall Attenuation Indoor Localization Algorithm . . . . .	9
3.2	WAFPL with different amount of walls . . . . .	13
3.3	Possible cases of Trilateration . . . . .	16
3.4	The two different cases of AGA . . . . .	17
3.5	AGA flowchart . . . . .	18
4.1	Signal processing performed in this thesis . . . . .	19
4.2	Setup of the site survey . . . . .	20
4.3	Setup of the corridor measurement . . . . .	21
4.4	Derivated path loss model of the corridor measurement . . . . .	21
4.5	Localization error analysis of the proximity algorithms . . . . .	23
4.6	Inside/Outside visualization of WC in the site survey . . . . .	24
4.7	Heatmap of the RSSs from AN <sub>4</sub> of the site survey . . . . .	25
5.1	Setup of the static/dynamic measurement . . . . .	30
5.2	CDF of the localization errors by WC in the static measurement . . . . .	31
5.3	Localized positions by WC in the static measurement . . . . .	31
5.4	Average performance of WAILA in the static measurement . . . . .	33
5.5	Higher localization errors when using lower RSSs . . . . .	34
5.6	CDF of the localization errors by WAILA in the static measurement . . . . .	35
5.7	Localized positions by WAILA (w/ Trilateration) in the static measurement . . . . .	36
5.8	CDF of the localization errors by WC in the dynamic measurement . . . . .	37
5.9	Localized positions by WC in the dynamic measurement . . . . .	38
5.10	Average performance of WAILA in the dynamic measurement . . . . .	39
5.11	CDF of the localization errors by WAILA in the dynamic measurement . . . . .	40
5.12	Localized positions by WAILA (w/ AGA) in the dynamic measurement . . . . .	41



# List of Tables

4.1	Path loss model derived from the corridor measurement . . . . .	22
4.2	Localization errors of the proximity algorithms (in meters) . . . . .	23
4.3	Room-level performances of the proximity algorithms . . . . .	24
4.4	Example of a Threshold Matrix . . . . .	26
4.5	Threshold Matrix derived of the site survey . . . . .	27
5.1	Parameters for WAILA . . . . .	32
5.2	Threshold Matrix derived of the static measurement . . . . .	32
5.3	Improvement of the range estimations in the static measurement . . . . .	33
5.4	Improvement of the range estimations in the dynamic measurement . . . . .	39
A.1	Anchor nodes . . . . .	47
A.2	Measurements . . . . .	47
A.2	Measurements . . . . .	48
B.1	Linear regression . . . . .	49
C.1	Anchor nodes . . . . .	51
C.2	Measurements . . . . .	51
C.2	Measurements . . . . .	52
D.1	Anchor nodes . . . . .	53
D.2	Measurements . . . . .	53
D.2	Measurements . . . . .	54
E.1	Localization errors of the static measurement (in meters) . . . . .	55
E.2	Localization errors of the dynamic measurement (in meters) . . . . .	56



# Chapter 1

---

## Introduction

Over the recent years, ubiquitous computing is becoming more and more of a reality. Thanks to the growing popularity of smart phones, the availability of mobile computing power has significantly increased. Now the next step is the evolution of so called smart homes. Current smart home applications often use ZigBee for the near field communication. Due to its low-power consumption it's suitable for low data rate applications that require long battery life. With increasing home automation, the user has access and full control over all connected devices at home. Additionally, procedures can be automated e.g. the light of a room can be automatically switched on or off, depending on the position of the user. Therefore, indoor localization is an important issue that needs to be solved to serve a best experience. Nevertheless, for indoor localization still does not exist any general solution as e.g. GPS does for the outdoor navigation. Due to shadowing effects it is difficult to find a universal indoor localization method. Hence, there are many different approaches that try to provide the best localization results when working in indoor environments.

In this work, we focus on the improvement of the indoor localization using the Received Signal Strength (RSS). With the help of a proper path loss model, we attempt to convert the RSSs measured from the ZigBee Network into matching range estimations. For this task, the Log-Normal Path Loss (LNPL) model is often used. Unfortunately this model does not consider any shadowing caused due to the indoor environment. Therefore, we select a more sophisticated model, called the Wall Attenuation Factor Path Loss (WAFPL). With this model the shadowing, which is caused due to walls can be included into the calculations of the path loss. Hence the range estimations are improved. By adding different steps before and after the path loss calculation, we create our own algorithm which increases the accuracy of user localizations in indoor environments.

Our algorithm is called Wall Attenuation Indoor Localization Algorithm (WAILA) and consists of three steps. The first step has the task of estimating a rough position of the user. We achieve this by using a range-free localization approach, as for example the Weighted Centroid. This position is then used in the second step to approximate the wall count and adapt these values to the WAFPL model. Additional algorithms we have added ensure the quality of the range estimations. In the last step, different localization algorithms e.g. Linear Least Square, Trilateration or Adaptive Geometric Algorithm, can be used with the range estimations to predict the final positions.

As the evaluation shows, our algorithm can improve the accuracy in indoor environments. To measure the improvement, we compare the performance of our algorithm with the Weighted Centroid. By analysing all versions of WAILA, we highlight the best localization algorithms, which can be chosen in the third step.

After this short introduction, the next Chapter 2 provides all theoretical basics, which are relevant for this thesis. Then, Chapter 3 explains in details the theoretical construction of our localization algorithm called Wall Attenuation Indoor Localization Algorithm. This algorithm is divided into three parts, which are explained step by step. In Chapter 4, we introduce initial two measurements. With the help of the data gathered from these measurements, we perform a preliminary experimental analysis in order to obtain different parameters and settings e.g. the Wall Attenuation Factor (WAF), proximity algorithm or Threshold Matrix (TM), for the next chapter. After the preliminary analysis, Chapter 5 introduces two new measurements and provides the evaluation of WAILA. We measure the performance of our algorithm as well as the performance of a range-free algorithm, the Weighted Centroid. Then we compare the performances for each measurement independently and analyse the results. Finally, Chapter 6 concludes with a brief summary of the results and an outlook for possible further work.

## Chapter 2

---

# Theoretical Background of Indoor Localization

In this chapter, all theoretical basics which are relevant to this thesis will be explained. It is divided into two parts. First, different path loss models are introduced in Section 2.1. Second, multiple localization algorithms, which are divided into range-free and range-based categories are explained in Section 2.2.

## 2.1 Signal Propagation

Path loss describes the attenuation of a transmitted signal at the time when it arrives at the receiver. This loss of signal strength can be due to many factors. For example, in free space, the signal can be attenuated due to the propagation distance. In practice, especially in indoor environments, it is still challenging to find an accurate model to map the distance to the corresponding path loss. As for example, the signal can be blocked by walls, which results in a large attenuation. Besides attenuation due to obstacles, multi-path propagation, because of reflected signals from different paths, introduces another inference to estimate the propagation distance based path loss. Such multi-path propagation can lead to a constructive or a destructive interference.<sup>1</sup>

The formula for the path loss according to the distance  $d$  is defined by [1]:

$$PL(d)_{[dBm]} = 10\gamma \log_{10} \left( \frac{P_t}{P_r} \right), \quad (2.1)$$

where  $P_t$  is the transmitted power,  $P_r$  is the received power and  $\gamma$  is the path loss exponent. In free space, the transmission power, which arrives at the receiver is described with the Friis free-space equation for the specific distance  $d$ ,

$$P_r = P_t \cdot G_t \cdot G_r \cdot \left( \frac{\lambda}{4\pi d} \right)^2, \quad (2.2)$$

---

<sup>1</sup>[http://en.wikipedia.org/wiki/Interference\\_\(wave\\_propagation\)](http://en.wikipedia.org/wiki/Interference_(wave_propagation))

where  $\lambda$  is the wavelength,  $G_t$  is the transmitter gain and  $G_r$  is the receiver antenna gain. A more generic path loss model is the Log-Normal Path Loss (LNPL) model, as following [1]:

$$\text{LNPL}(d)_{[dBm]} = \text{PL}(d_0)_{[dBm]} + 10\gamma \log_{10} \left( \frac{d}{d_0} \right) + X_\sigma. \quad (2.3)$$

The parameter  $\gamma$  is used to define the path loss exponent. For indoor applications,  $\gamma$  generally takes values from 2 to 4. A value of  $\gamma = 2$  is often used to describe the free space path loss model [1].  $\text{PL}(d_0)$  is the path loss at reference distance  $d_0$ . Usually this reference distance  $d_0$  is set to 1 meter [1]. Furthermore  $X_\sigma$  denotes the random zero mean Gaussian variable added to the formula. It reflects the shadowing fading due to obstacles. In practice, it is still challenging to accurately model the shadowing fading and it actually introduces large bias. Therefore, some other models try to better represent the shadowing fading.

The Wall Attenuation Factor Path Loss (WAFPL) model is a path loss model, which accounts the shadowing effect of walls and is more suitable for indoor environments. Its formula is given by [2; 3],

$$\text{WAFPL}(d)_{[dBm]} = \text{PL}(d_0)_{[dBm]} + 10\gamma \log_{10} \left( \frac{d}{d_0} \right) + \hat{\beta} + \mathcal{N}, \quad (2.4)$$

where  $\mathcal{N}$  is the noise without any attenuation due to walls and  $\hat{\beta}$  is defined as:

$$\hat{\beta} = \begin{cases} h \cdot \text{WAF} & \text{for } h < C \\ C \cdot \text{WAF} & \text{for } h \geq C \end{cases} \quad (2.5)$$

where  $h$  is the amount of walls between the anchor node and the target and  $C$  is the maximal allowed amount of walls in the environment. Depending on the count of walls, the WAFPL model applies an additional path loss  $\hat{\beta}$ . Such path loss consists of the amount of walls multiplied by a previously estimated WAF. The Wall Attenuation Factor (WAF) value defines how much a single wall can attenuate the strength of the signal. If  $h$  is greater than the maximal allowed amount of walls set in  $C$ , the WAF value will be simply multiplied by the limiting value  $C$ .

## 2.2 Localization Algorithms

Indoor localization algorithms can be classified as either range-based or range-free localization. Range is defined as the distance between the sender and receiver.

Range-based localization needs to first extract range from certain signal parameters e.g. RSS and time information like TOA or TDOA. Then the users can be located by certain localization algorithms based on the range information and coordinates of the anchor nodes (ANs) as for example with Trilateration.

Range-free localization does not need to obtain any range information for localization. Such algorithms can directly process the RSS or time information to localize the user, e.g. proximity or fingerprinting.

### 2.2.1 Range Free Localization

Generally, range-free methods are easier to implement compared to range-based methods, because they do not need range information. Therefore, these methods are considered as more cost-effective. However, not all approaches are able to achieve satisfying accuracies. Fingerprinting promise higher accuracy, but comes with high labour costs and is very time consuming [4; 5].

#### Nearest Neighbour

The Nearest Neighbour (NN)<sup>2</sup> algorithm simply selects the location of the  $i$ -th anchor node  $AN_i$  with the strongest signal denoted as  $RSS_i$ . Let the variable  $RSS$  be defined as the vector of all signal strengths,

$$RSS = [RSS_1, \dots, RSS_n]^T, \quad (2.6)$$

where  $RSS_i$  belongs to  $AN_i$ . Thus, the position of the Nearest Neighbour is defined as:

$$NN(RSS) = \langle x, y \rangle_{AN_i}, \text{ with } \max(RSS) = RSS_i, \quad (2.7)$$

where  $\langle x, y \rangle_{AN_i}$  are the coordinates of the  $i$ -th anchor node.

#### Nearest Room Neighbour

As an enhancement of the Nearest Neighbour, we propose to use the centre of the corresponding room instead of the anchor node itself. Most of the time, the anchor nodes are positioned near a wall or a corner. When analysing a position at the other end of a room, the error is equal to the full length of the corresponding room. Thus, by using the centre of the room, the maximum localization error is reduced to the half of the length of the room. Therefore, instead of the anchor node, the Nearest Room Neighbour (NRN) that we created by ourselves, selects the centre of the room where the anchor node is located in. The formula of the NRN is as following:

$$NRN(RSS) = \langle x, y \rangle_{RC_i}, \text{ with } \max(RSS) = RSS_i, \quad (2.8)$$

where  $\langle x, y \rangle_{RC_i}$  is the centre of the room containing the  $i$ -th anchor node.

#### Centroid

The Centroid algorithm calculates the arithmetic mean position of a polygon with  $n$  vertices, whereas the position of an anchor node is a vertex. In case of a triangle ( $n = 3$ ), the Centroid is the intersection of the three medians of the triangle. The general formula for any  $n$  is the following [7]:

---

<sup>2</sup>bases on [http://en.wikipedia.org/wiki/K-nearest\\_neighbors\\_algorithm](http://en.wikipedia.org/wiki/K-nearest_neighbors_algorithm) where  $k = 1$

$$\text{Centroid}(\text{AN}) = \frac{\langle x, y \rangle_{\text{AN}_1} + \langle x, y \rangle_{\text{AN}_2} + \cdots + \langle x, y \rangle_{\text{AN}_n}}{n}, \quad (2.9)$$

where  $\langle x, y \rangle_{\text{AN}_i}$  are the coordinates of the  $i$ -th anchor node and  $n$  defines the count of anchor nodes used.

### Weighted Centroid

To improve the Centroid algorithm, weights are added to each anchor node. Therefore, a weight function  $w$  needs to be defined. With the help of the calculated weights, the centroid position is moved towards the anchor nodes, which are assigned with the biggest weights. The formula for the Weighted Centroid (WC) algorithm is as following [6]:

$$\text{WC}(w, \text{AN}) = \sum_{i=1}^n w_i * \langle x, y \rangle_{\text{AN}_i}, \quad (2.10)$$

where  $w_i$  is the weight calculated by the weight function  $w$  for the  $i$ -th anchor node and AN is the vector containing all anchor nodes. We introduce such a weight function  $w$  in Chapter 3.

### Fingerprinting

Fingerprinting algorithms can be divided into two steps, offline training and online positioning [15]. For offline training, the mobile device needs to move across the whole interesting area, recording RSS in every training position. Then the RSS values and corresponding training positions are stored in a database. For online positioning, after measuring the RSS values, a certain matching algorithm needs to be adopted to find the best matching training position in the database and finally locate the target.

Fingerprinting algorithms can provide high localization accuracy, but also require very intense labour work to build the database. The database is prone to changes of the surrounding environment and requires frequently updates [13; 14].

## 2.2.2 Range Based Localization

Range-based localization methods needs to first measure range information. Therefore, range-based algorithms are often more complex compared to the range-free approaches. However, they potentially achieve better localization accuracy [16].

### Statistical Approach

When solving the localization in a statistical manner, an optimization problem is formulated. By constructing multiple equations, the solution is searched numerically in order to achieve the smallest error. For example the Non-Linear Least Square (NLS) estimates the position by finding  $\langle \hat{x}, \hat{y} \rangle$  when solving the following equation:

$$\langle \hat{x}, \hat{y} \rangle = \operatorname{argmin}_{x,y} \sum_{i=1}^N \left[ \sqrt{(x_i - x)^2 + (y_i - y)^2} - d_i \right]^2 \quad (2.11)$$

where  $N$  is the amount of anchor nodes used to localize the position,  $d_i$  is the estimated distance and  $\langle x, y \rangle$  as the known coordinates of the anchor nodes [8].

A linear approximation of the NLS algorithm is the Linear Least Square (LLS). LLS linearizes the problem formulation, by adding a new intermediate value into the formulation. Hence it needs less computational power compared to NLS. The procedure of LLS will be explained in detail in Section 3.4, where we use it for the final localization [9; 8].

### Geometrical Approach

Most often, when using a geometrical approach, the concept of Trilateration<sup>3</sup> is used. Trilateration is the process of locating a target by using circles (or spheres in three-dimensional space) with the estimated distances  $d_i$  as the radius. By finding an intersection among all circles, the final position is localized inside this area. The implementation of this Trilateration algorithm is shown in details in Section 3.4, which is also used in our algorithm.

It is possible due to the influence of multi-path, measuring errors or falsely estimated distances, that no intersection can be found. On the other hand it is also possible, that the resulting intersection is too big to provide an accurate localization.

Therefore, an improved Trilateration algorithm called Adaptive Geometric Algorithm (AGA) is provided by the authors of [10]. AGA is able to solve the issues of having none or too big intersection areas. More details of the Adaptive Geometric Algorithm will be presented in Section 3.4.

---

<sup>3</sup><http://en.wikipedia.org/wiki/Trilateration>



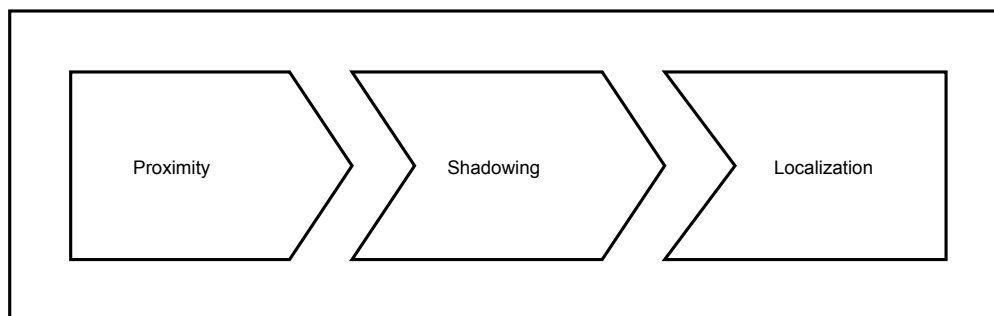
## Chapter 3

# Developed Indoor Localization Algorithm

As a part of this research, we develop an improved localization algorithm, based on the Wall Attenuation Factor Path Loss model. The idea is to improve the localization accuracy by accounting the amount of walls, which are included in the path loss between the sender and the receiver. By taking the amount of walls into the calculation of the range measures, improved distance estimations can be provided. Our algorithm is called Wall Attenuation Indoor Localization Algorithm and will be referred to as WAILA in future.

WAILA combines range-free as well as range-based localization approaches. First, range-free methods are used to establish an initial position. Second, range-free methods are performed in order to improve the localization by using additional information like the layout of the environment or WAF. Because of its division into range-free and range-based parts and to provide a better overview, the algorithm is divided into 3 steps as shown in Figure 3.1.

**Figure 3.1:** Wall Attenuation Indoor Localization Algorithm



The first step is called *Proximity*. In this step, a range-free algorithm is proposed to estimate a rough location of the user because of its simplicity. Some typical range-free algorithms can be selected, such as the Weighted Centroid or other range-free methods described in Section 2.2.1.

The next step is called *Shadowing*. Based on the rough location from the first step and with the help of the predefined Wall Attenuation Factor (WAF), we adopt the Wall Attenuation Factor Path Loss model as seen in Chapter 2 to improve the accuracy of the derived range values. This step runs through multiple stages. First, the count of walls is approximated for each link between the target and each anchor node. Then the path loss model is modified by the shadowing values.

Finally, the distance values are improved by an additional algorithm we've created, called the *Threshold* algorithm.

In the last step, which is called *Localization*, the final position of the user is estimated. For this purpose, one of the implemented range-based localization algorithms can be chosen from, such as LLS, Trilateration or AGA. By combining these three steps, WAILA tries to improve the indoor localization by considering the wall attenuation influence on RSS.

### 3.1 Preparation

Since plenty of RSS are collected over a certain time-frame and the localization algorithms require an explicit value to locate the target, we need to select a proper method to aggregate the measured RSS values to an effective value. Therefore, multiple statistics can be used, such as the min, max, median or mean value. In our work, we use the mean value.

Accordingly, a  $RSS_i$  is calculated from all measured RSS for each anchor node  $AN_i$  as following:

$$RSS_i = \frac{1}{m} \cdot \sum_{j=1}^m RSS_{i,j}, \quad (3.1)$$

where  $RSS_{i,j}$  is the  $j$ -th measurement collected by the anchor node  $AN_i$ . Hence we can define the vector RSS uses as following:

$$RSS = [RSS_1, \dots, RSS_n]^T, \quad (3.2)$$

where  $RSS_i$  is the mean RSS of the  $i$ -th anchor node.

### 3.2 Step 1: Proximity

In this step, an initial position, which is close to the real position, should be estimated. To perform this task, a range-free method is used. Therefore, the wall attenuation contained in the Received Signal Strength will be ignored for the moment. WAILA offers four choices of range-free algorithms as introduced in Chapter 2, which are:

- Nearest Neighbour
- Nearest Room Neighbour
- Centroid
- Weighted Centroid

As mentioned before, all of these algorithms are very simple and need little information about the ranging. While the first three exclusively work with the RSS, the Weighted Centroid additionally requires a weight function  $w$ . In this work, we take use of the Log-Normal Path Loss model (without any Gaussian noise) to predict the estimated distances. The estimated distances can then be used for further weight calculations. However, it needs to be mentioned that these weights can also be calculated without any range-based approach. Hence the weights are calculated according the following formula [6]:

$$w_i = \frac{\frac{1}{d_i}}{\sum_{j=1}^n \frac{1}{d_j}}, \quad (3.3)$$

where  $n$  is the amount of anchor nodes,  $w_i$  is the weight for anchor node  $AN_i$  and  $d_i$  is the estimated distance between  $AN_i$  and the target. Finally, the estimated position  $\langle x, y \rangle_{estimated}$  is calculated by one of these four proposed algorithms. The result is then forwarded to the next step for further calculations.

### 3.3 Step 2: Shadowing

In the second step, the focus lies on the calculation of distances from every anchor node to the user's position. First, the count of walls for each link needs to be calculated. Second, the existing WAFPL model is completed by adding additional information regarding signal attenuation. Finally, the predictions from the upgraded path loss model are further checked, based on the layout of the environment. If any prediction is considered as invalid, the threshold algorithm is adopted and performs a correction.

#### 3.3.1 Wall Approximation

Based on the knowledge about the layout of the surrounding environment, it is possible to approximate the amount of walls between the user and each anchor node. Therefore, the previously estimated position can be used as an assumption of the real position. By simply drawing a straight line between each anchor node and the estimated position, the direct connection among the sender and receiver is shown. Thus every wall that intersects this line possibly attenuates RSS. Hence the amount of walls can be approximated by counting the amount of intersections for each line. This way a vector  $h$  containing the count of walls to every anchor node is created.

$$h = [h_1, \dots, h_n]^T, \quad (3.4)$$

where  $n$  is the number of anchor nodes used and  $h_i$  is the number of walls between the estimated position  $\langle x, y \rangle_{estimated}$  and the anchor node  $AN_i$ . This vector  $h$  is forwarded to the next stage of the shadowing step.

### 3.3.2 Path Loss Model

As shown in section 2.1, the wall shadowing  $\hat{\beta}$  from the WAFPL model is constructed as the following (when  $h \leq C$ , where  $C$  is the wall limiting value):

$$\hat{\beta} = h \cdot \text{WAF}, \quad (3.5)$$

where  $h$  is the approximated amount of walls between the anchor node and the target and WAF is the previously defined Wall Attenuation Factor.

RSSs that are attenuated by walls, are received less powerful at the anchor nodes, resulting in oversized estimated distances by the path loss model. The Wall Attenuation Factor Path Loss model tries to adjust this effect by adding an additional path loss value specified by  $\hat{\beta}$ . As shown in Figure 3.2, by adding the final shadowing component  $\hat{\beta}$  to the path loss formula the WAFPL model is shifted on the y-axis. With the help of the approximated amount of walls, we are able to estimate a  $\hat{\beta}$  for each link individually. Hence, the curve is shifted down along the y-axis with bigger  $\hat{\beta}$  values. In this way attenuated RSSs are mapped to distances that fit the real distances more likely.

Since we know only the RSS value instead of the path loss for an unknown distance, the formula needs to be extended as following [13]:

$$\text{RSS}(d) = T_p - \text{WAFPL}(d) \quad (3.6)$$

$$\text{RSS}(d) = T_p - \left( \text{PL}(d_0) + 10\gamma \log_{10} \left( \frac{d}{d_0} \right) + \hat{\beta} + \mathcal{N} \right) \quad (3.7)$$

where  $T_p$  is the transmit power. In terms of simplicity, we propose to ignore the noise  $\mathcal{N}$  in the future calculations. Hence, we can further simplify the equation as following:

$$\text{RSS}(d) = T_p - \left( \text{PL}(d_0) + 10\gamma \log_{10} \left( \frac{d}{d_0} \right) + \hat{\beta} \right) \quad (3.8)$$

$$\text{RSS}(d) = T_p - \text{PL}(d_0) - 10\gamma \log_{10} \left( \frac{d}{d_0} \right) - \hat{\beta} \quad (3.9)$$

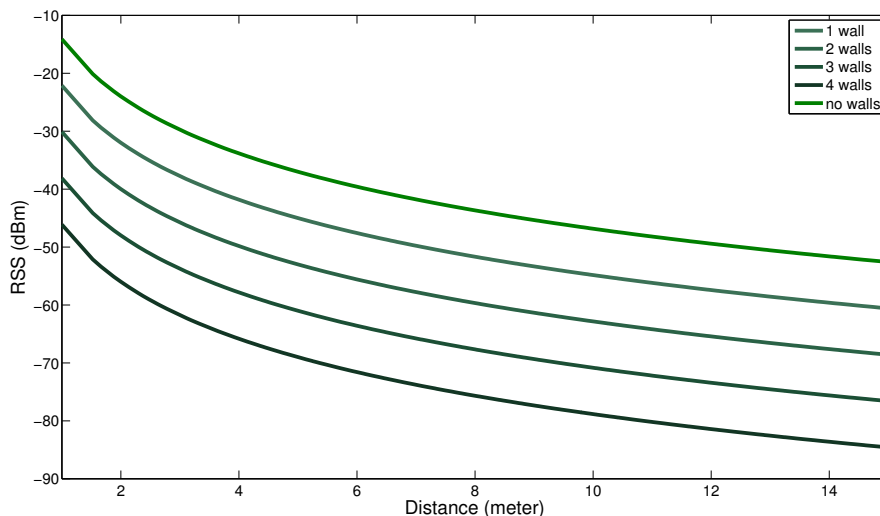
Because the transmit power  $T_p$  as well as the path loss at the reference distance  $\text{PL}(d_0)$  are both fixed values, we set  $\alpha = T_p - \text{PL}(d_0)$ . Additionally, we define  $\beta = 10 \cdot \gamma$ . Since the reference distance is 1 meter, the simplified equation is:

$$\text{RSS}(d) = \alpha - \beta \cdot \log_{10}(d) - \hat{\beta} \quad (3.10)$$

$$\text{RSS}(d) = \alpha - \beta \cdot x - \hat{\beta} \quad (3.11)$$

where further  $x = \log_{10}(d)$ . Given this simplified formula, we are able to solve the equation for  $d$  with the help of the previously defined  $\alpha$  and  $\beta$ .

**Figure 3.2:** WAFPL with different amount of walls



Finally the path loss model can be used in order to compute the distances between the user and the anchor node. Hence, we get:

$$\hat{d} = [\hat{d}_1, \dots, \hat{d}_n]^T, \quad (3.12)$$

where  $\hat{d}_i$  is the distance to the  $i$ -th anchor node.

### 3.3.3 Threshold

It is possible that some of the evaluated distances  $\hat{d}_i$  might be not reasonable. This can be due to many reasons. For example a false estimated position in the first step can lead to an incorrect approximation of the amount of the walls. It leads to a wrong shift in the path loss curve and estimates an inaccurate distance assumption. Other possible sources of errors are heavily attenuating furniture that cannot be included in the WAFPL model. Hence an additional check of the distances  $\hat{d}$  needs to be performed.

Therefore, we have created an algorithm called *Threshold*. This algorithm checks if a calculated distance  $\hat{d}$  is valid or not. Such validation is performed depending on the approximated amount of walls  $h_i$ . The decision is determined with the help of a previously calculated Threshold Matrix (TM). This  $(C + 1) \times 3$  matrix defines for each measurable amount of walls<sup>1</sup> an interval of valid distances. The first column specifies the amount of walls and is simply provided for a easier understanding. Then the second column of the matrix consists of the valid minimal distances for each count of walls, whereas the third column defines the possible maximal distances. When running the algorithm, it looks up the corresponding minimal and maximal values depending on the measured amount of walls. If the calculated distance  $\hat{d}_i$  is located inside this interval, it is considered as valid. However, if the value exceeds the specific interval,

<sup>1</sup>from 0 to  $C$ , where  $C$  defines the maximum allowed amount of walls in Equation 2.5

the calculated distance will be set to the nearest boundary value. This way erroneous distance values can be corrected, by being adapted to a certain threshold.

$$\text{Threshold}(\hat{d}, h, TM) = \hat{d}' = [\hat{d}'_1, \dots, \hat{d}'_n]^T \quad (3.13)$$

---

**Algorithm 1** Threshold

---

**Input:** All calculated distances  $\hat{d}$ , All approximated counts of walls  $w$ , Threshold matrix  $TM$

**Output:** Final distances  $\hat{d}'$

```

1: for each pair  $\langle \hat{d}_i, w_i \rangle$  from  $\hat{d}$  and  $w$  do
2:   if  $w_i > C$  then
3:      $w_i \leftarrow C$  {Apply condition from WAFPL}
4:   end if
5:    $min \leftarrow$  minimum of  $TM[w_i]$ 
6:    $max \leftarrow$  maximum of  $TM[w_i]$ 
7:   if  $\hat{d}_i$  is NOT inside interval  $[min, max]$  then
8:     if  $\hat{d}'_i < min$  then
9:        $\hat{d}'_i \leftarrow min$ 
10:    end if
11:    if  $\hat{d}'_i > max$  then
12:       $\hat{d}'_i \leftarrow max$ 
13:    end if
14:  else if  $\hat{d}_i$  is inside interval  $[min, max]$  then
15:     $\hat{d}'_i \leftarrow \hat{d}_i$ 
16:  end if
17: end for
18: return  $\hat{d}'$ 

```

---

Finally the improved distance vector  $\hat{d}'$  is calculated and can be forwarded to the last step.

### 3.4 Step 3: Localization

In the final step the target is located based on the improved distance information. Therefore, we provide a set of different range-based algorithms. The available algorithms are the following:

- Linear Least Square [9]
- Trilateration
  - using the three closest/strongest anchor nodes
  - using all  $n$  anchor nodes
- Adaptive Geometric Algorithm [10]

Only one of the available algorithms can be selected to locate the user for each measurement. Finally, after the chosen algorithm is executed, the position  $\langle x, y \rangle_{final}$  is found and returned as the final result of WAILA.

In the following sections, the different range-based localization algorithms are explained in details.

### 3.4.1 Linear Least Square

The Linear Least Square (LLS) is an linearized approach of the NLS estimation. It contains a set of equations as following [9]:

$$z_i^2 = (x - x_i)^2 + (y - y_i)^2, \text{ for } i = 1, \dots, N \quad (3.14)$$

where each of these equations is considered as a circle. Now one of the equations  $0 < r \leq i$  is selected as a reference measurement and is subtracted from all the other equations. Hence we can transform the formula into a matrix formulation [9]:

$$Al = p, \quad (3.15)$$

where  $l = [x, y]^T$ , with:

$$A = 2 \cdot \begin{bmatrix} x_1 - x_r, y_1 - y_r \\ \vdots \\ x_{r-1} - x_r, y_{r-1} - y_r \\ x_{r+1} - x_r, y_{r+1} - y_r \\ \vdots \\ x_n - x_r, y_n - y_r \end{bmatrix}, \quad (3.16)$$

$$p = \begin{bmatrix} z_r^2 - z_1^2 - k_r + k_1 \\ \vdots \\ z_r^2 - z_{r-1}^2 - k_r + k_{r-1} \\ z_r^2 - z_{r+1}^2 - k_r + k_{r+1} \\ \vdots \\ z_r^2 - z_n^2 - k_r + k_n \end{bmatrix}, \quad (3.17)$$

where  $k_i = x_i^2 + y_i^2$  and  $r$  is the reference equation.

Given the formula in Equation 3.15, we can solve it for  $l$  as following[9]:

$$\hat{l} = (A^T A)^{-1} A^T p = [x, y]^T \quad (3.18)$$

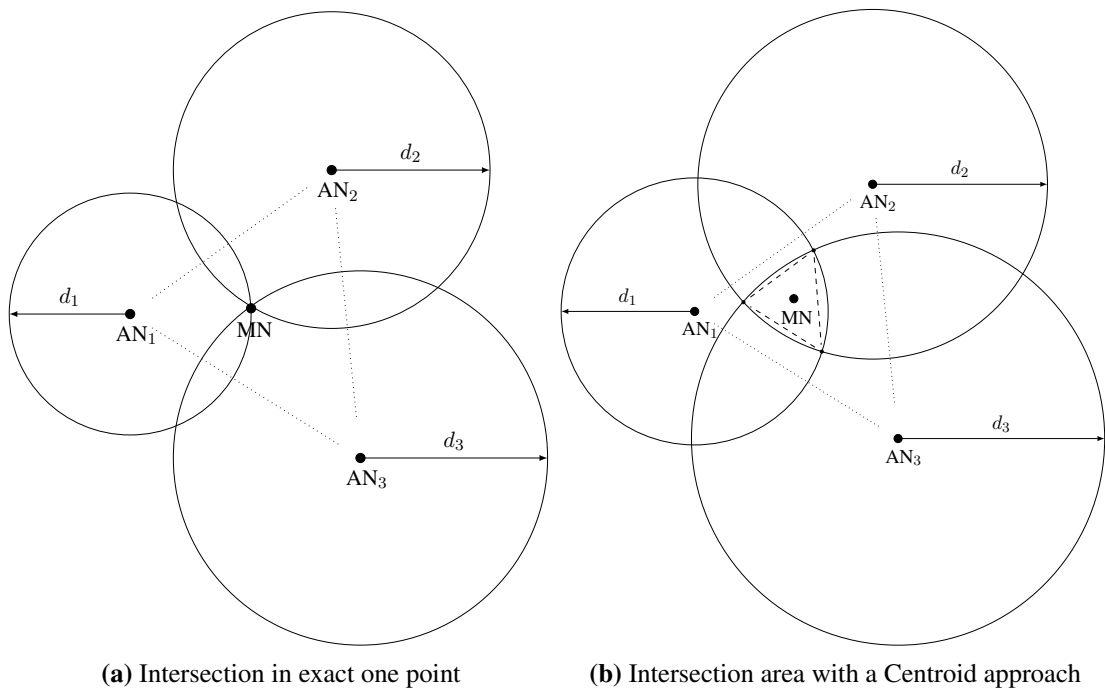
### 3.4.2 Trilateration

Trilateration is the process of localizing the user with the help of distance measurements. Because at least three distinct distances need to be known, it is often referred to as Trilateration. Depending on the dimension, Trilateration is performed either with spheres or circles. Since we focus on analysing only one floor, we use the 2-dimensional notation with circles.

As shown in Figure 3.3a, three anchor nodes are used. The value  $d_i$  is the distance between the target and the  $i$ -th anchor node. By drawing the circles, the position of the user is estimated at the intersection of the three circles, which is denoted as mobile node (MN) in such figures. If the intersection of all circles doesn't precisely result in one position, the coordinates of the intersections between each pair of circles can be used for further localization. By using the Centroid algorithm, the centroid location from the different intersections can be estimated as the user's position as shown in Figure 3.3b.

Trilateration (Trilat) can also be used with more than three anchor nodes. Therefore, we speak about Trilateration with  $n$  anchor nodes or simply refer to as TrilatN.

**Figure 3.3:** Possible cases of Trilateration



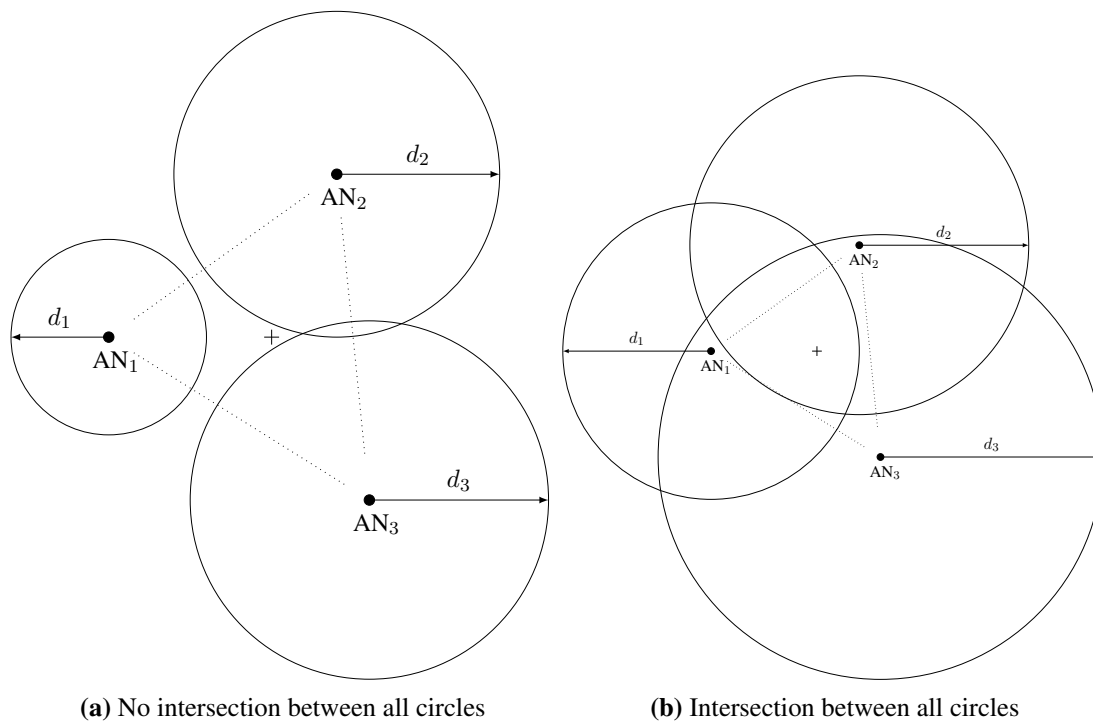
### 3.4.3 Adaptive Geometric Algorithm

The Adaptive Geometric Algorithm (AGA) is an enhancement of the Trilateration algorithm that is performed with only three anchor nodes. Its goal is to reduce the relevant area, i.e. the intersection area, to a minimum. AGA distinguishes between two different cases. Either there

is no existing intersection between all three circles as shown in Figure 3.4a or an intersection<sup>2</sup> exists between all three circles as shown in Figure 3.4b. Depending on the situation, a different value for the factor  $k$  is selected, which can be less or greater than one. With the help of this factor, all circles are either linearly downscaled or linearly up scaled.

As shown in the flowchart in Figure 3.5, in the first case, where an intersection between all three circles exists,  $k$  is set to less than one ( $k < 1$ ). Now all three radii are iteratively multiplied by the factor  $k$  until the smallest possible intersection area is found. This is the case, when any further decrease of the radii leads to the state where an intersection cannot be found anymore. In this way the sizes of all circles are linearly decreased. In case that no intersection can be found,  $k$  is selected as greater than one ( $k > 1$ ). Thus the circle radii are increased until a minimal intersection area is found by the algorithm [10].

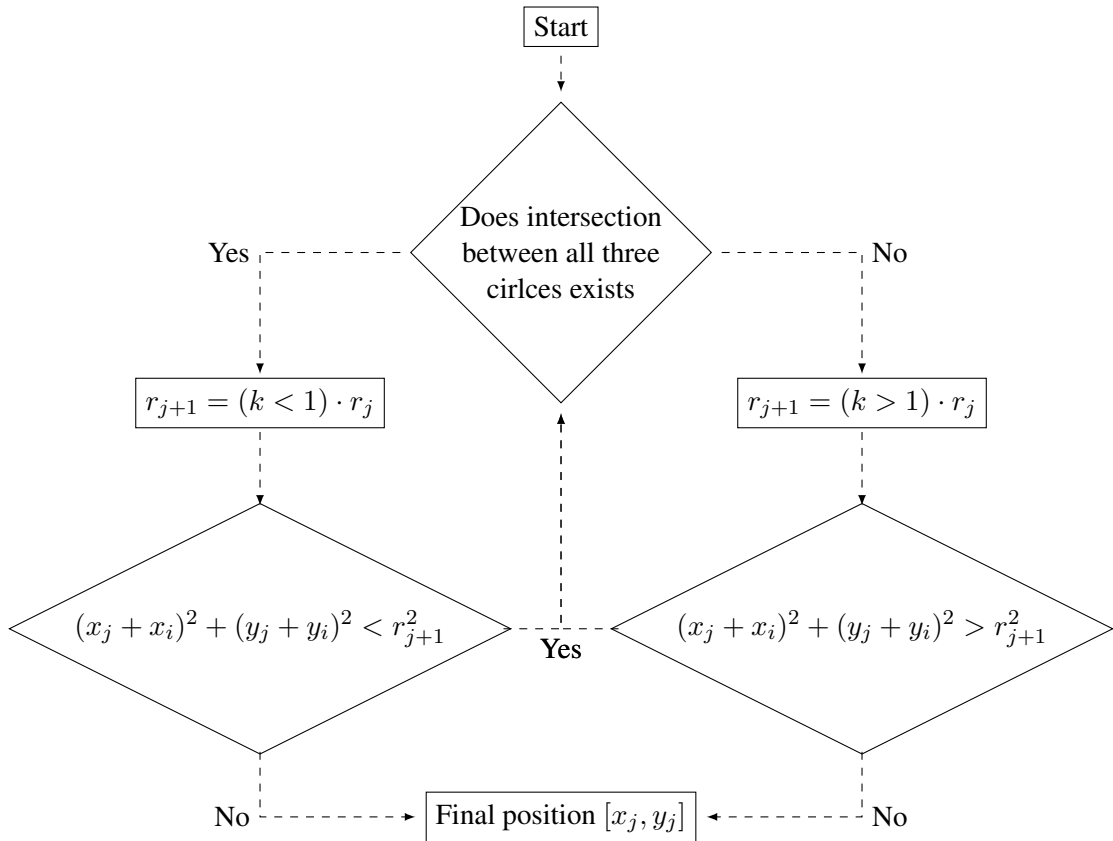
**Figure 3.4:** The two different cases of AGA




---

<sup>2</sup>possibly rather large

**Figure 3.5:** AGA flowchart



Source: A Novel Enhanced Positioning Trilateration Algorithm Implemented for Medical Implant In-Body Localization. [10]

## Chapter 4

# Preliminary Experimental Analysis

In this chapter, we introduce some preliminary measurements. Based on the output from these measurements, we determine multiple values, e.g. WAF, path loss model values or Threshold Matrix, which are used for the final evaluation of WAILA in Chapter 5.

### 4.1 Practical Measurements

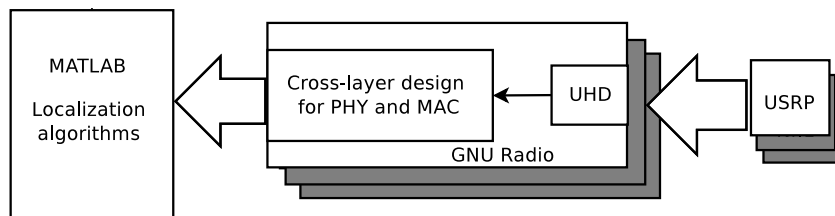
#### 4.1.1 Hardware

For the hardware one TelosB sensor as well as multiple Universal Software Radio Peripheral (USRP) devices are used. The USRP N210 receivers are placed in the examined area in order to log the signal strength of the transmitted packages. These receivers are referred to as anchor nodes (ANs). In parallel, the sensor node, which periodically sends packages, is placed at the different positions.

#### 4.1.2 Software

To evaluate our proposed system, we design a passive system based on Software Defined Radio (SDR), which can overhear IEEE 802.15.4 signals and extract RSS from the captured message. Signal processing is implemented in GNU Radio, which is utilized for demodulation and packet reconstruction. RSS information of each packet is passed to MATLAB for the localization algorithm.

**Figure 4.1:** Signal processing performed in this thesis

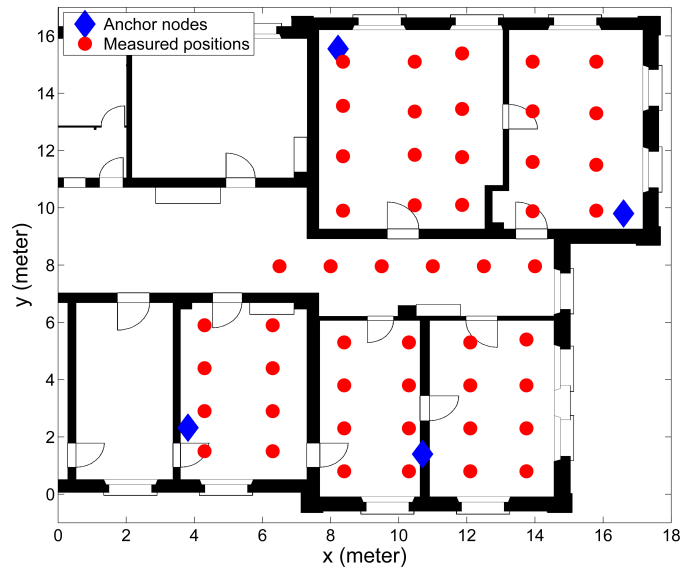


### 4.1.3 Environment

The measurements are all conducted on parts of the second floor of the IAM building of the University of Bern as for example shown in Figure 4.2. This area is composed out of 8 different rooms, which are all connected with one corridor in the centre of this layout.

### 4.1.4 Site Survey

**Figure 4.2:** Setup of the site survey



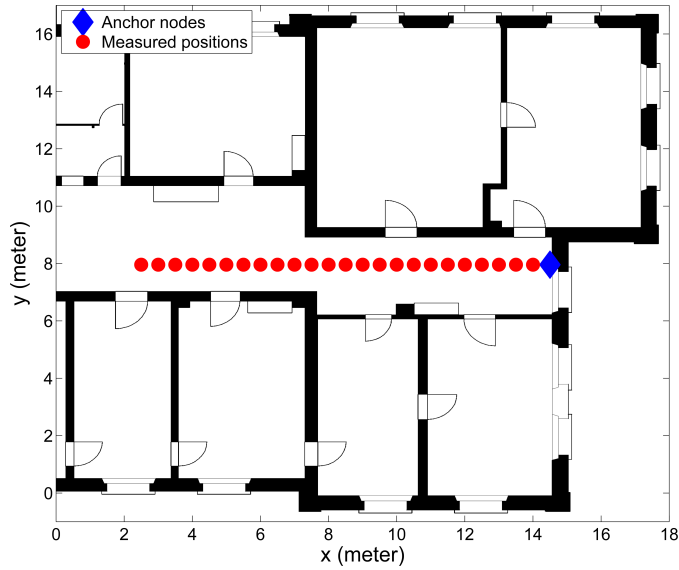
In the first measurement, 50 positions are measured for their RSS as shown in Figure 4.2 with the red markers. The blue markers show the positions of the four distributed anchor nodes. Because the measurement is recorded on a weekend, it is considered to be recorded in a static environment. This means that none of the measured RSS is disturbed by any moving obstacles, as for example by people walking around or working in their offices. Hence this measurement should be well-suited for the analysis of the signal distribution in a static indoor environment.

### 4.1.5 Corridor Measurement

In order to investigate the path loss in line of sight (LOS) condition over a large distance, we conduct another measurement. In this measurement, only one anchor node is used. The anchor node is located at the end of the corridor, which is shown by a blue marker in Figure 4.3. Starting at the position of the anchor node, measurements are taken by every 0.5 meter step away from it. Thus there are in total 24 measurement positions over a distance of 12 meters, which are highlighted by the red markers.

The purpose of this measurement is that the  $\alpha$  and  $\beta$  from the simplified equation shown in Section 3.3.2 can be calculated, since there is no attenuation  $\hat{\beta} = 0$ . The measurement is also

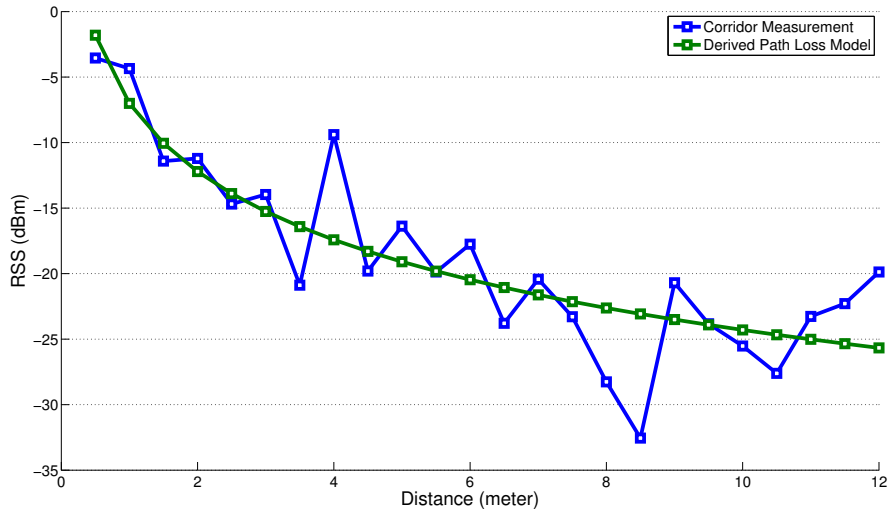
**Figure 4.3:** Setup of the corridor measurement



recorded over the weekend with nobody working in the office at this time. Therefore, it can be considered to be a static environment as the site survey.

## 4.2 Path Loss Model Derivation

**Figure 4.4:** Derivated path loss model of the corridor measurement



With the help of the corridor measurement shown in Figure 4.3 and by performing a linear regression, we can derive the coefficients  $\alpha$  and  $\beta$  of the path loss model for the specific indoor

environment. The formula we use to describe the WAFPL model in Section 3.3.2 is as following:

$$\text{RSS}(d) = \alpha - \beta \cdot x - \hat{\beta}, \quad (4.1)$$

where we set  $x = \log_{10}(d)$ . Because the corridor measurement is recorded without any walls in line of sight, the  $\hat{\beta}$  is equal to zero for every measured position. In order to solve for the  $\alpha$  and  $\beta$  values, a linear regression is performed on the corridor measurement dataset. The complete calculations can be found in Appendix B. Thus the  $\alpha$  and  $\beta$  values can be approximated and are shown in Table 4.1.

**Table 4.1:** Path loss model derived from the corridor measurement

<b>PL <math>\alpha</math></b>	-7.0077
<b>PL <math>\beta</math></b>	17.2908
<b>PL Exponent <math>\gamma</math></b>	1.729

It is striking, that the path loss exponent  $\gamma$  with 1.7291 is very low for an indoor environment. The reason is that no walls or other objects block the signal. It is also possible that due to the architecture of the corridor, a tunnelling effect may enhance the overall signal strength. Hence it is very similar to the propagation in free space. Path loss that results from attenuation will be added later with the help of the  $\hat{\beta}$ .

For comparison, additionally the path loss exponent is calculated based on the site survey measurement in Section 4.1.4. Because the deviation of the site survey already contains all signal attenuation, the path loss exponent is much higher. It was found at 3.26745, which is a much more suitable value for an indoor environment. However this value cannot be used in the Wall Attenuation Factor Path Loss model, since the attenuation would be calculated twice into the equation due to the  $\hat{\beta}$ .

### 4.3 Proximity Algorithm

In the first step of the WAILA in Section 3.2, we proposed to use one of the following range-free algorithms:

- Nearest Neighbour
- Nearest Room Neighbour
- Centroid
- Weighted Centroid

Since only one algorithm can be used, we analyse the data of the site survey in order to find the best performance of these range-free approaches. The first three range-free algorithms can be directly used with RSS. However, the Weighted Centroid uses the path loss model we derived in section 4.2 in order to calculate the weights.

**Figure 4.5:** Localization error analysis of the proximity algorithms

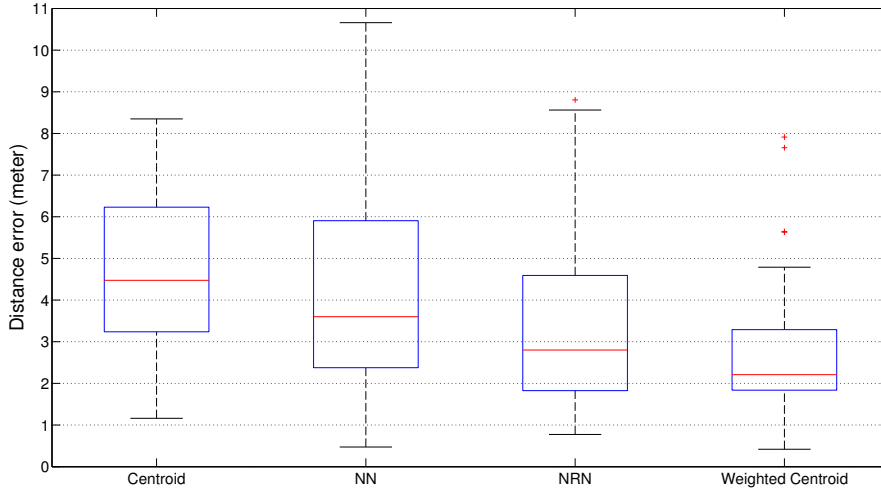


Figure 4.5 shows a box plot with all 50 localization errors for each algorithm. We can find that the Weighted Centroid performs best. It is capable to achieve about 75% of all positions within a maximal error below 3.5 meters. Also its median value of 2.21 meters is considerably better than the Nearest Room Neighbour algorithm with 2.8 meters. The mean value as well as the median value over all 50 errors are shown in Table 4.2.

**Table 4.2:** Localization errors of the proximity algorithms (in meters)

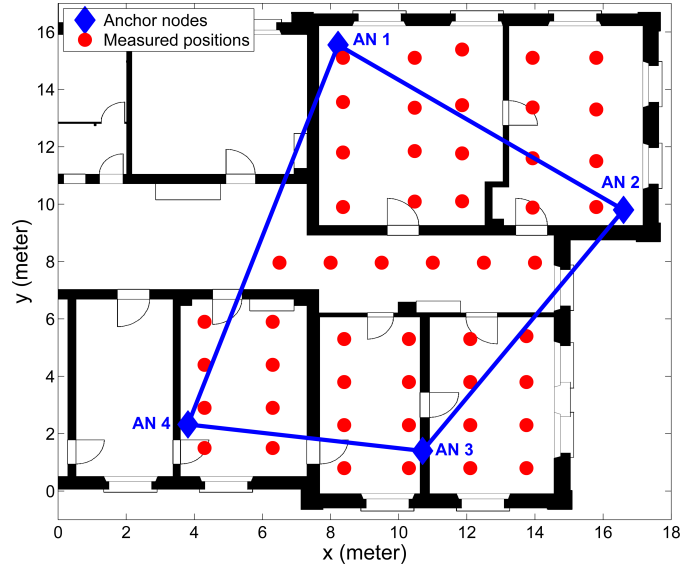
Algorithm	Centroid	NN	NRN	WC
<b>Average error</b>	4.5363	4.279	3.334	2.687
<b>Median error</b>	4.4750	3.6005	2.8014	2.2094

Except the Weighted Centroid, all used algorithms can only locate the target at certain fixed positions. For example NN estimates the target at one of the anchor nodes position. Hence its localization accuracy is bound to the amount of anchor nodes used. However, the estimated position of the Weighted Centroid can be tuned by the weights and is therefore not bound to certain fixed positions.

Another indicator of the performance is the accuracy of the room level. Since the estimated position will be used to determine the amount of walls, it is very important that the estimation is located at least in the correct room. Otherwise the approximation of the walls might compute a wrong number of walls. This can then lead to future miscalculation. Because the Nearest Neighbour and the Nearest Room Neighbour always locate the estimation inside the same room, only one of them has to be analysed.

In Table 4.3 the amount of measurement located within the correct rooms are counted. It needs to be remembered, that the Weighted Centroid can locate only inside the area stretched by the positions of the anchor nodes. As it can be seen in Figure 4.6, almost 20 measured positions are not located inside this area. Therefore, these positions have a higher chance of

**Figure 4.6:** Inside/Outside visualization of WC in the site survey



being mapped into an incorrect room. Furthermore the position of the anchor node 3, which is located between the room at the bottom in the middle and the bottom right room, is problematic. The measurements in the room right to it are most likely incorrectly placed and mapped into an wrong room.

**Table 4.3:** Room-level performances of the proximity algorithms

	All AN	Without AN <sub>4</sub>	Without AN <sub>3</sub>	Without AN <sub>2</sub>	Without AN <sub>1</sub>
<b>Centroid</b>	4/50	6/50	12/50	6/50	8/50
<b>NN/NRN</b>	28/50	20/50	21/50	24/50	19/50
<b>WC</b>	30/50	24/50	28/50	23/50	24/50

The worst performance is achieved by the Centroid algorithm. This algorithm always selects the centre position between the three anchor nodes with the strongest signal. Hence only four different positions can be localized. Due to the fact that these positions are located mostly in the corridor, almost all estimations are incorrect. In this case all positions are mapped onto the same location. Hence at least all positions of one room are located in the correct room.

The NN as well as the NRN algorithm achieve quite good results since they are able to locate all measured positions inside a room with an anchor node correctly. Because 4 out of 6 rooms<sup>1</sup> are equipped with an anchor node, both algorithms can locate 56% of the positions within room level. If one of the anchor nodes is removed, the performance drops as shown in Table 4.3.

The best performance is again achieved by the Weighted Centroid algorithm. It reaches a room level of about 60% for all the measured positions. As the only algorithm, it is capable to locate positions in the corridor correctly. When anchor nodes are removed, the performance

<sup>1</sup>including the corridor

tend to decrease less compared to NN and NRN. A possible reason for this is that the Weighted Centroid is not bound to a certain amount of fixed position. Therefore, it is not necessarily the case that all localizations inside the room where the anchor node is removed are distorted.

Based on these result, the Weighted Centroid will be used in the proximity step for all future evaluations of WAILA.

## 4.4 Wall Attenuation

According to the Wall Attenuation Factor Path Loss model, a WAF value, which describes the attenuation of a single wall, needs to be known. In this thesis, all walls are treated as the same and are calculated with the same WAF. Even though there are small differences between some of them, generally they have the same thickness and consist of the same material.

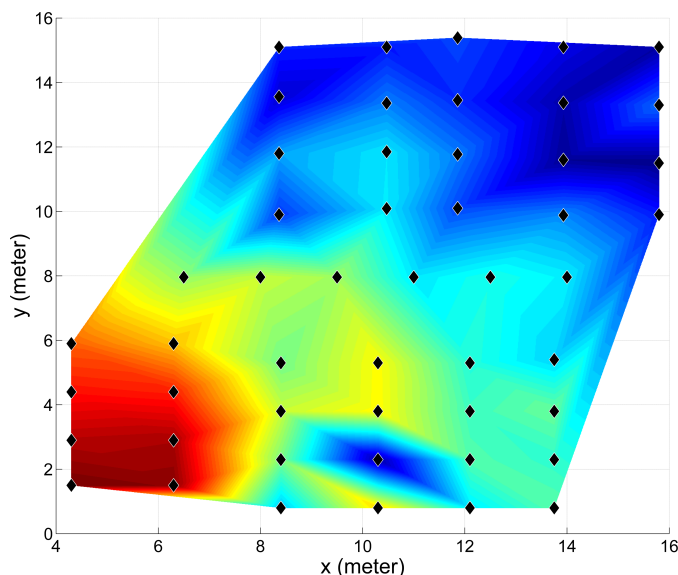
$$\text{RSS}(d) = \alpha - \beta \cdot \log_{10}(d) - \hat{\beta} - \mathcal{N}, \quad (4.2)$$

with  $\hat{\beta} = h \cdot \text{WAF}$  where  $h \leq C$ . Hence the formula can be solved for WAF:

$$\text{RSS}(d) - \alpha + \beta \cdot \log_{10}(d) = -(h \cdot \text{WAF}) - \mathcal{N} \quad (4.3)$$

Unfortunately, walls don not cause the only attenuation that exists. Objects like tables, computers, chairs and so on provide additionally not negligible influences. Thus  $\mathcal{N}$  cannot be simply ignored when looking for WAF. Otherwise the found factor could be estimated too big, resulting in position localizations further away.

**Figure 4.7:** Heatmap of the RSSs from AN<sub>4</sub> of the site survey



In Figure 4.7 the distribution of the Received Signal Strengths captured by the fourth anchor node is shown. Warm colours indicate high RSS, whereas cold colours as blue indicate very low RSS. All colours between the measurement positions are interpolated and don't reflect the exact RSS. However the effect of the walls stands out strongly, especially when comparing with Figure 4.2.

As shown in Figure 4.7, the variance of RSS in different areas is very high in the site survey measurement. The attenuation between an anchor node and targets that are located right behind the nearest wall varies from 6 dBm up to almost 30 dBm. Most often the values range between 10 dBm to 13 dBm. Because these values also contain attenuation that is not caused due to walls, WAF must be lower. It should be noted that this type of attenuation is not added to our calculations, since it is caused due to objects in LOS, which will not be considered in this model. A similar research study performed in the same area also used a WAF, where the author selected a value of 9 dBm [17].

Finally, we choose WAF to be 8 dBm for all future calculations.

## 4.5 Threshold

In Section 3.3.3, we introduced the threshold algorithm. In order to use it, a minimal and maximal distance for each count of walls needs to be known. This piece of information can be displayed in form of a matrix, as shown in Table 4.4.

**Table 4.4:** Example of a Threshold Matrix

Number of walls	Minimum distance	Maximum distance
0	0 m	5 m
1	4 m	7 m
...	...	...
$C$	$C_{min}$	$C_{max}$

To create such a Threshold Matrix, an additional algorithm, called the threshold finder has been created. This algorithm takes use of the knowledge about the environment and the setup of the conducted measurement. Its goal is to create an assumption of the most probable minimal and maximal distance with  $i$  walls in-between the link. Therefore, the algorithm analyses every link between each anchor node and every measured position from the analysed measurement. With the knowledge of the environment, the algorithm determines the real amount of wall for every link. Additionally, it calculates the straight-line distance  $d$  between the two positions. Then it temporally stores all the distances depending on their amount of walls. By doing this, the algorithm creates a hash table, where the keys  $k$  are the count of walls among each link. Hence, every key  $k_i$  points to a vector that contains all distances  $d$ , which exactly contain  $i$  walls in-between the link. When this hash table is completed, the algorithm starts with the selection process. For every possible amount of walls, thus for every key  $k_i$  it selects the minimal and maximal distance from the corresponding vector. For easier handling, it builds a  $(C + 1) \times 3$

matrix<sup>2</sup>, where the first column states the amount of walls, the second the minimum and the third the maximum distance.

In pseudo code, the threshold finder looks as shown in Algorithm 2.

---

**Algorithm 2** Threshold Finder

---

**Input:** All measured positions  $M$ , All anchor nodes  $AN$

**Output:** Threshold matrix  $TM$

```

1:  $H \leftarrow$  new hash table {can contain multiple values for a key}
2: for  $m \leftarrow$  each element of  $M$  do
3:   for  $an \leftarrow$  each element of  $AN$  do
4:      $w \leftarrow$  Walls between  $m$  and  $an$ 
5:     if  $w > C$  then
6:        $w \leftarrow C$ 
7:     end if
8:      $d \leftarrow$  Distance from  $m$  to  $an$ 
9:     insert  $d$  into  $H$  at key  $w$ 
10:  end for
11: end for
12:  $TM \leftarrow$  new  $(C + 1) \times 3$  matrix
13: for  $k \leftarrow$  every key of  $H$  do
14:    $min_k \leftarrow$  minimal value from  $H$  at key  $k$ 
15:    $max_k \leftarrow$  maximum value from  $H$  at key  $k$ 
16:    $TM(k, 2) \leftarrow min_k$ 
17:    $TM(k, 3) \leftarrow max_k$ 
18: end for
19: return  $TM$ 

```

---

From the site survey measurement, the threshold finder algorithm computed the Threshold Matrix shown in Table 4.5.

**Table 4.5:** Threshold Matrix derived of the site survey

Number of walls	Minimum distance	Maximum distance
0	0.4725 m	6.5538 m
1	0.7545 m	10.2662 m
2	3.1852 m	15.7526 m
3	5.2424 m	15.3458 m
4	7.7421 m	17.5191 m

Because the result of the threshold finder depends on the setup of the measured coordinates. We propose to redo the calculation each time we conduct a measurement with a new setup of the anchor nodes.

---

<sup>2</sup>the variable  $C$  states the maximal allowed amount of walls, defined in Section 2.1



## Chapter 5

---

# Evaluation of WAILA

In this chapter we evaluate the performance of the WAILA algorithm. Therefore, we implement the WAILA algorithm in our own MATLAB framework, which includes the proposed steps from Chapter 3. Additionally, we create various scripts for gathering and visualizing the gained information. Besides the parameters defined in the preliminary analysis in Chapter 4, two new measurements are conducted for this evaluation.

We evaluate our proposed WAILA algorithm based on the different localization algorithms used in the third step. Furthermore, we additionally evaluate the performance of the Weighted Centroid for comparison. Therefore, we use the algorithm explained in Section 2.2.1 without any integration of the WAFPL. The evaluation is performed for each measurement and first starts with the Weighted Centroid followed by the analysis of the WAILA algorithm.

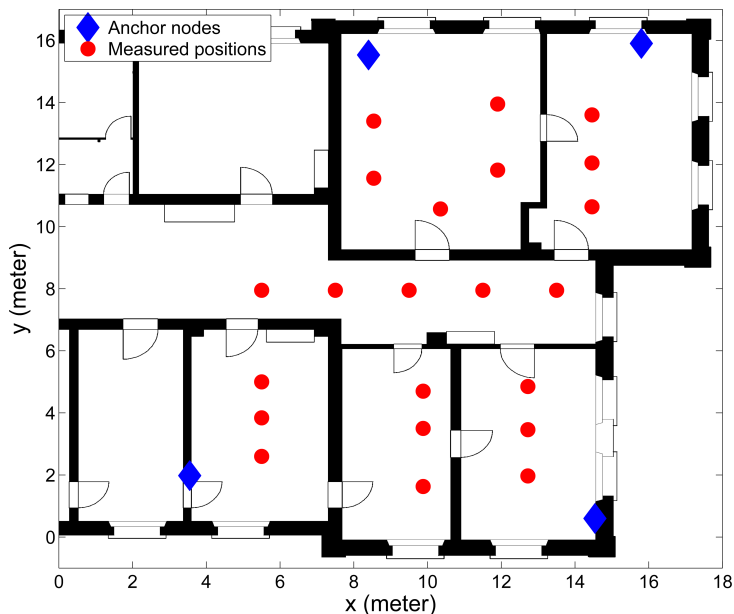
### 5.1 Evaluation Measurements

In addition to the site survey and corridor measurement shown in Section 4.1.4 and Section 4.1.5, we conduct two new measurements. Both measurements are again conducted in the second floor of the IAM building of the University of Bern. As shown in Figure 5.1, 22 positions are tested in each measurement. Altogether, 4 anchor nodes are distributed over the examined area. To ensure that both recordings are comparable, they share the same layout of the measured position as well as the location of the anchor nodes.

The positions of two anchor nodes are slightly changed compared to the site survey shown in Figure 4.2. The reason for this rearrangement is the higher coverage achieved when running the Weighted Centroid algorithm. As explained in Section 4.3, the Weighted Centroid is only able to locate positions inside the polygon area, which is stretched by the anchor nodes positions. Therefore, the covered surface could be raised from around  $100m^2$  in the site survey to almost  $135m^2$ .

The first measurement is recorded over the weekend, while the second measurement is conducted during the working time. Therefore, we refer to the first measurement as the static measurement and the second one as the dynamic measurement. In the static measurement, all RSS values are recorded under the same conditions, but the dynamic measurement adds a new level of complexity. With people walking around in the offices, the signal propagation can change every moment. Thus, the measured RSS from the dynamic measurement might be recorded with

**Figure 5.1:** Setup of the static/dynamic measurement



different signal distributions. This makes the localization more difficult than it is in the static measurement.

## 5.2 Performance in the Static Measurement

First we analyse the data in the static measurement. Initially the performance of the Weighted Centroid is evaluated in Section 5.2.1. Then we study the results of WAILA and compare them with the Weighted Centroid in Section 5.2.2.

### 5.2.1 Weighted Centroid

We begin with the Weighted Centroid whose performance we use as a reference performance for our algorithm.

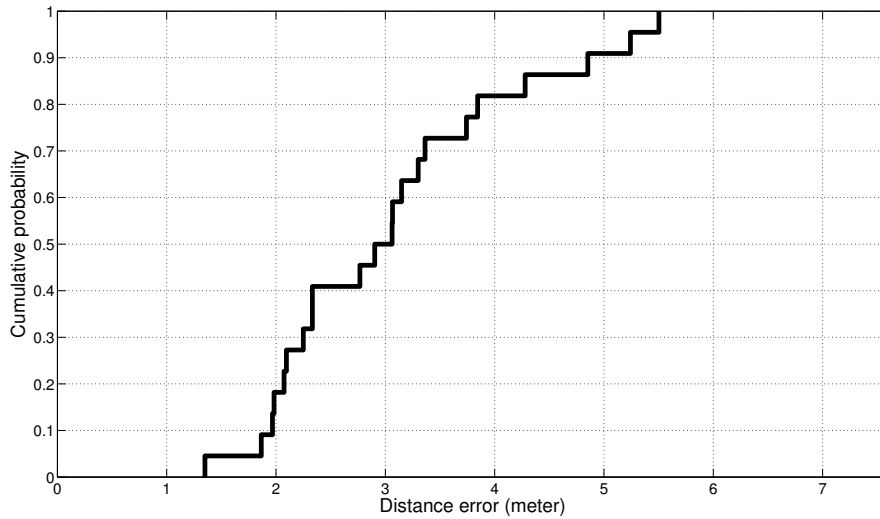
As explained in Section 2.2.1, the Weighted Centroid needs a weight function, which defines a weight for each anchor node. Since we created one in Section 3.2, it is convenient to just reuse it. Because the weight function needs a path loss model, we also take use of the corridor path loss model derived in Section 4.2.

#### Location Errors

When calculating with all 22 positions, the average localization error measures approximately 3.1 meters. The minimum localization is around 1.3 meters, whereas the maximum localization error measures almost 5.5 meters. Considering the room-level accuracy, the Weighted Centroid

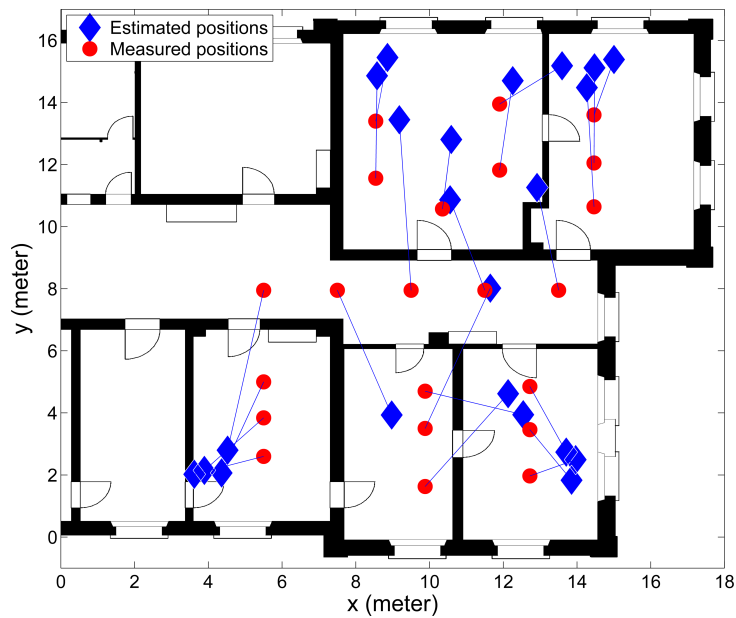
achieves a result of around 60%. Only positions that are inside a room containing an anchor node can be matched to the correct room as it is shown in Figure 5.3.

**Figure 5.2:** CDF of the localization errors by WC in the static measurement



In Figure 5.2 the localization errors are plotted in form of a Cumulative Distribution Function (CDF). About 50% of all errors are smaller than 3 meters and almost 75% can be still located below 3.5 meters. Generally, the localization errors are evenly spread. However, a minor change at around the 80% mark of all localization error can be noticed in the CDF.

**Figure 5.3:** Localized positions by WC in the static measurement



The estimated positions by the Weighted Centroid, which are marked as the blue diamonds, are shown in Figure 5.3. The red markers show the real position and the blue lines the resulting localization error. As explained in Section 4.3 regarding the Weighted Centroid in the site survey, the performance behaves similarly to this result. Based on the Figure 5.3, we can find that the estimated positions are pulled strongly towards the different anchor nodes. This clearly shows, even though achieving a good performance, the Weighted Centroid is a range-free method and limited in its accuracy.

## 5.2.2 Wall Attenuation Indoor Localization Algorithm

Eventually, we evaluate the performance of WAILA. In order to run the algorithm, we need certain parameters. With exception of the threshold matrix, all necessary parameters are already defined in the preliminary analysis in Chapter 4. These parameters are listed in Table 5.1.

**Table 5.1:** Parameters for WAILA

<b>WAF</b>	8 dBm
<b>C</b>	4 walls
<b>WAFPL coefficients</b>	$\begin{bmatrix} \alpha & = & -7.0077 \\ \beta & = & 17.2908 \end{bmatrix}$

To obtain the threshold matrix, we simply use the Threshold Finder shown in Section 4.5. With help of this algorithm we can directly derive a matrix from the static measurement. The found threshold matrix is displayed in Table 5.2.

**Table 5.2:** Threshold Matrix derived of the static measurement

<b>Number of walls</b>	<b>Minimum distance</b>	<b>Maximum distance</b>
0	0.4725 m	6.5538 m
1	0.7545 m	10.2662 m
2	3.1852 m	15.7526 m
3	5.2424 m	15.3458 m
4	7.7421 m	17.5191 m

Furthermore, we select the Weighted Centroid algorithm in the proximity step, as justified in Section 4.3. In the localization step of WAILA, we propose to test all four available algorithms. Hence we evaluate WAILA by running it multiple times, each time with a different algorithm performing in the third step.

### Range Errors

As a part of our algorithm, we improve the localization accuracy by improving the range estimations. This process is explained in detail in the second step of WAILA in Section 3.3. The enhancement of the range estimations is split into three parts. First, a range estimation is performed with the path loss model without the shadowing component  $\hat{\beta}$ . As shown in Table 5.3,

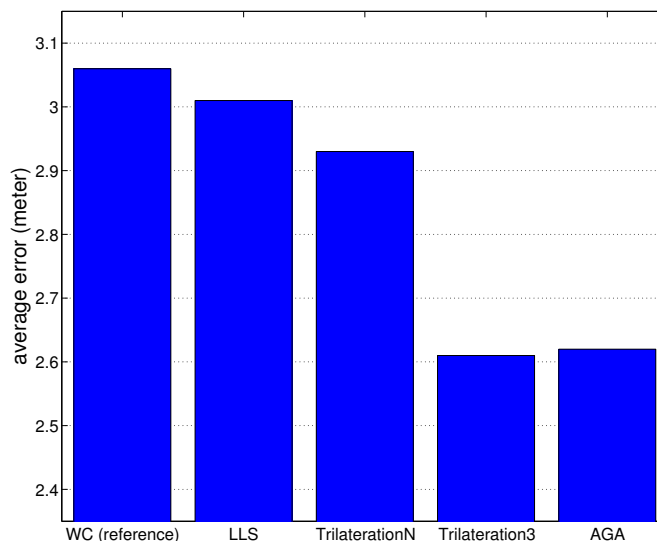
in the static measurement, the first step results in a mean ranging error of about 70 meters and a maximal error of 1323 meters. Such large ranging errors are because the path loss model is measured by the corridor measurements and the wall attenuation effect is not yet considered.<sup>1</sup> After adding the shadowing component  $\hat{\beta}$  to the path loss model, the ranging errors are greatly reduced. The new mean error is reduced to about 21.5 meters and the maximum ranging error is improved by more than 700% to around 185.5 meters. However, these values are still unsuitable for indoor localization, mainly due to two reasons. First, in the first step of WAILA, the Weighted Centroid may generate an inaccurate initial position, which results in an error in the approximation of walls. Second, since the distance and path loss model follow an exponential model, a small variation for the RSS values from the ANs will result in a large ranging error. Therefore, the threshold algorithm in the last step helps binding the maximum error to a certain limit. After that, the new mean error measures only 2.1 meters, whereas the maximum ranging error is bound to just 9.35 meters.

**Table 5.3:** Improvement of the range estimations in the static measurement

Step	mean	max
Path loss	69.794 m	1323.2 m
Path loss & $\hat{\beta}$	21.506 m	185.484 m
Path loss & $\hat{\beta}$ & Threshold	2.146 m	9.35 m

## Location Errors

**Figure 5.4:** Average performance of WAILA in the static measurement



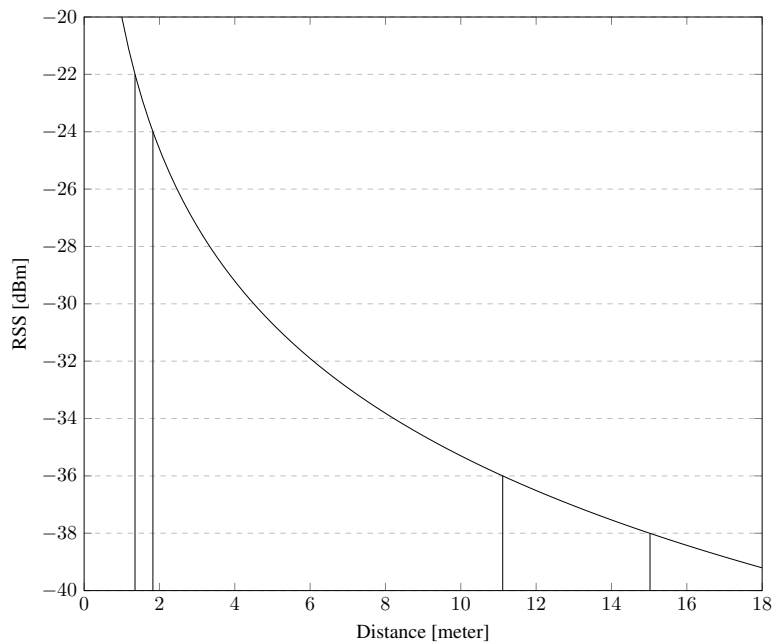
<sup>1</sup>Such high errors can be explained due to the logarithmic form of the path loss model.

In Figure 5.4, the achieved average localization errors are shown. Since there are four different algorithms used in the third step of WAILA, we label every performance by the specific algorithm used in this step. As a reference value, the first bar shows the performance of the Weighted Centroid from Section 5.2.1. The best average localization accuracy is achieved by AGA and the Trilateration versions of WAILA. The Trilateration reaches an average error of around 2.61 meters, whereas AGA closely follows with 2.62 meters accuracy. The two worse performing versions of WAILA are the ones using the Trilateration with  $n$  anchor nodes and the Linear Least Square. However, both achieve an improvement compared to the Weighted Centroid. While LLS achieves a localization error of only 3 meters in average, the TrilatN algorithm is able to accomplish an accuracy of at least 2.93 meters.

CDF of WAILA is shown in Figure 5.6. First we compare LLS and TrilatN. Both algorithms start with very small localization errors and then grow almost similarly with increasing errors. At around 50% the performance of TrilatN clearly overcomes LLS. Generally LLS shows a more linear growth compared to TrilatN.

Perhaps one reason for the poorer performance of TrilatN and LLS can be the amount of anchor nodes used for the localization. While the better performing algorithms such as AGA and Trilateration only work with exactly 3 anchor nodes, the other two use as many as they can have. Even though we just use 4 anchor nodes in total, this additional anchor node can already have a negative impact.

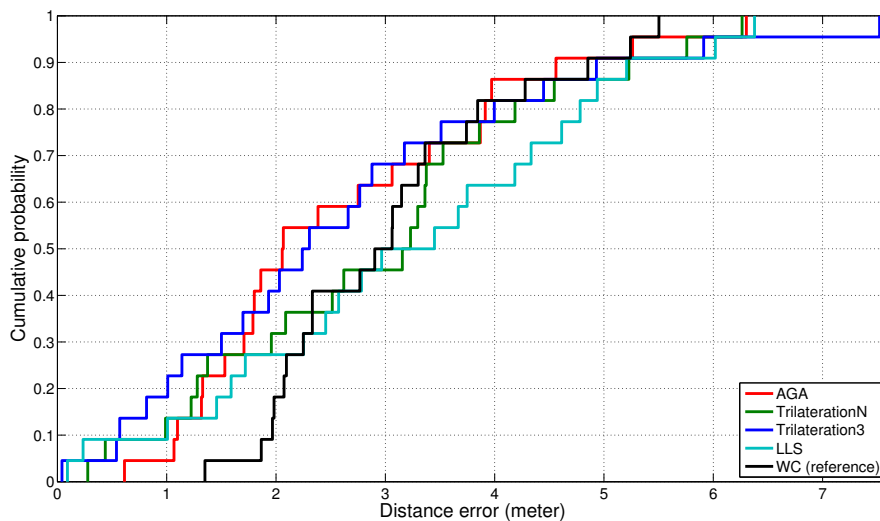
**Figure 5.5:** Higher localization errors when using lower RSSs



To explain this potential issue we have a look at Figure 5.5. Due to the logarithmic form of the path loss model we use, lower RSS tend to cause bigger ranging errors, thus bigger localization errors. For example a RSS of -23 dBm with a general noise of 1 dBm can take any

value from -22 dBm to -24 dBm. Such interval of possible RSS values is then mapped by the path loss model onto a distance between approximately 1.35 and 1.8 meters. Hence we receive an interval of the length of less than 0.5 meter. When we do the same experiment with a lower RSS of for example -37 dBm and the same noise as before, the possible distances vary between circa 11 to 15 meters. Now we have a possible distance interval of a length of about 4 meters. Therefore, signal data from anchor nodes far off must be handled more carefully. Since in the LLS and TrilatN all anchor nodes are treated equally, this may not add any improvement and cause larger errors.

**Figure 5.6:** CDF of the localization errors by WAILA in the static measurement



Henceforth, we analyse the performance of AGA and Trilateration by the results shown in the CDF in Figure 5.6. Both versions of WAILA start with a localization error below 1 meter. While the Trilateration is able to start off at a minimal error of about 0.04 meter, AGA has more troubles and achieves a smallest localization error of 0.61 meter. From there on, AGAs performance is generally poorer than the one of the Trilateration. At approximately 35% this relationship turns as the localization errors of the Trilateration increase slightly faster than the errors of AGA. Even though AGA starts with larger localization errors, it is capable to keep the maximal error down in relation to Trilateration. Therefore, its maximal localization error of 6.3 meters is almost 1.3 meters smaller compared with the one of Trilateration.

Eventually, we can say that Trilateration spreads its errors over a larger interval, but also achieves to localize more close estimations. On the other hand, AGA starts with larger localization errors, but is capable to keep the errors closer together in terms of a smaller maximal localization error. Despite all the differences, both algorithms greatly improve the localization compared to the LLS or TrilatN versions of WAILA. Hence we only compare them with the performance of the Weighted Centroid from Section 5.2.1.

In general, both algorithms show a great improvement compared to the Weighted Centroid. The average localization error is improved by 0.45 meter when using WAILA. The minimal error of 1.34 meters achieved by the Weighted Centroid is heavily decreased to almost zero

(0.04 meter) when comparing with the Trilateration. However, the maximum localization error cannot be reduced by any of our versions. Nevertheless, both algorithms compensate for this effect with less larger errors.

In Figure 5.6, we compare the performances with the distribution of the Weighted Centroid, represented by the black curve. The gap between WC and AGA/Trilat is most conspicuous. It starts at the bottom of the y-axis and goes up to about 70%. All localization errors in this area are improved by the two versions of WAILA. For the remaining 30% of the localization errors, the Weighted Centroid as well as our two versions of WAILA achieve about the same accuracy.

**Figure 5.7:** Localized positions by WAILA (w/ Trilateration) in the static measurement

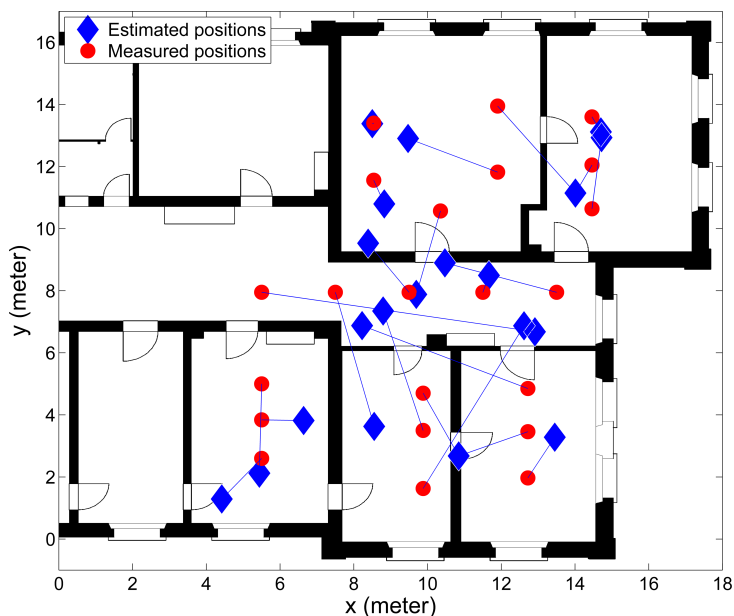


Figure 5.7 shows the localization errors when using WAILA with Trilateration. As before in the analysis of the Weighted Centroid, the red markers indicate the real positions, the blue markers show the estimated positions and the blue lines display the localization errors for each pair of points. When we compare it with the localization results of the Weighted Centroid, we can see that it does not directly follow a pattern like in Figure 5.3. However, the localizations are not simply random as they may appear. The estimations are generally closer to the real positions and most importantly not just pulled towards the closest anchor node. Hence the performance is more interesting compared to the WC localization, in which the user is estimated always close to a certain anchor node. Even though this behaviour can have a negative effect on the accuracy of the room-level<sup>2</sup>, the room-level is increased to about 64%. In addition, it can be noted that the largest localization errors are mostly located in rooms, which do not have a LOS with any anchor node.

<sup>2</sup>depending on the ratio of AN's and rooms and their distribution, the WC achieves a high coverage more easily

## 5.3 Performance in the Dynamic Measurement

Finally the data in the dynamic measurement, which is conducted during the working hours is analysed. Since the human body has a big influence considering attenuation, RSS tends to diversify stronger compared to the static measurement.

### 5.3.1 Weighted Centroid

Again the Weighted Centroid is analysed first to obtain a reference value for the performance of WAILA later on. It is run with the same weight function as in the previous analysis with the static measurement in Section 5.2.1.

#### Location Errors

In average the Weighted Centroid achieves an accuracy of 3.16 meters. The smallest localisation error amounts approximately 1 meter and the largest error is about 8.7 meters. When counting the room-level accuracy, the Weighted Centroid achieves almost 60% in this dynamic measurement.

**Figure 5.8:** CDF of the localization errors by WC in the dynamic measurement

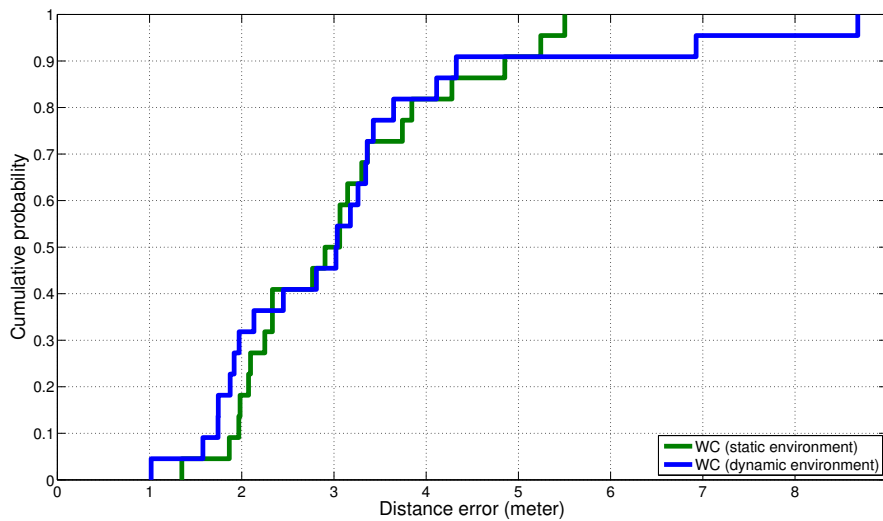
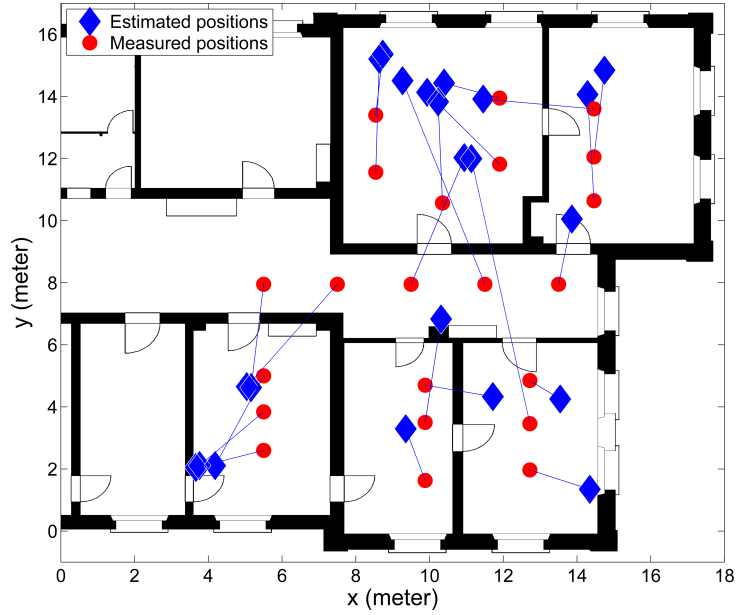


Figure 5.8 shows CDF of all 22 localization errors as the blue curve. Additionally the green curve shows CDF of WC from the static measurement, described in Section 5.2.1. Obviously, the Weighted Centroid is a very stable algorithm, comparing the performances from the static and the dynamic measurement. Again it behaves very similar as in the first analysis. Only some of the largest localization errors are increased.

This time, the estimated positions of the targets are pulled less towards the anchor nodes. As shown in Figure 5.9, some of the localized positions are placed more randomly. This randomness is most likely added due to the changing signal distribution caused by the people working in their

**Figure 5.9:** Localized positions by WC in the dynamic measurement



offices and walking around. However, the Weighted Centroid is capable to maintain its general localization accuracy.

### 5.3.2 Wall Attenuation Indoor Localization Algorithm

Eventually we evaluate WAILA with the data in the dynamic measurement. As in the static measurement, the used parameters are the same as shown in Table 5.1. Since both measurements share the same setup, the threshold finder algorithm explained in Section 4.5 delivers the same matrix as shown in Table 5.2. Hence the results of the dynamic measurement are fully comparable to the ones of the static measurement.

#### Range Errors

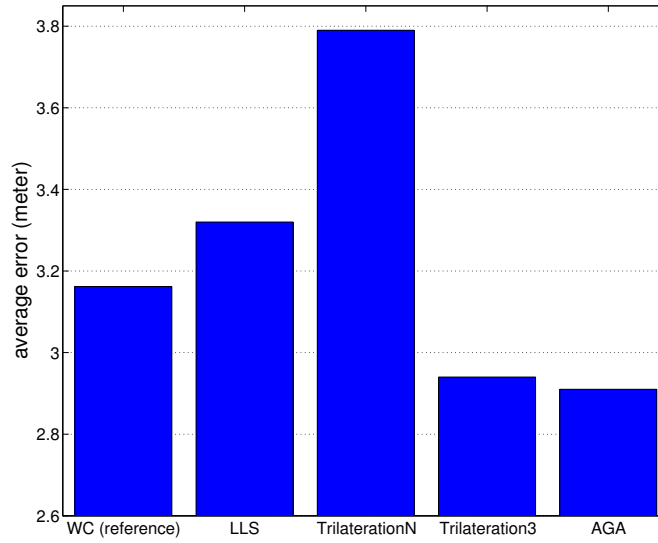
First, we have a short look at the range estimations. When the path loss model without any shadowing component  $\hat{\beta}$  is used, a mean range error of about 74 meters is achieved as shown in Table 5.4. The maximal range error measures approximately 1943 meters. The reason for these enormous values is the logarithmic structure of the path loss model. As long as RSSs are not adjusted, unreasonable signal strengths cause the path loss model to produce extreme distance assumptions. After we add the shadowing component  $\hat{\beta}$  to the path loss model, the values settle to circa 16 meters as the mean ranging error and circa 74 meters as the maximum error. Since these values are inapplicable for the localization process, the threshold algorithm applies the limiting values. After the last step, the range estimations are suitable for the further usage. We now achieve a mean error of 2.35 meters and a maximal range error of 9.35 meters.

**Table 5.4:** Improvement of the range estimations in the dynamic measurement

Step	mean	max
Path loss	74.131 m	1943.3 m
Path loss & $\hat{\beta}$	15.966 m	74.218 m
Path loss & $\hat{\beta}$ & Threshold	2.35 m	9.35 m

## Location Errors

**Figure 5.10:** Average performance of WAILA in the dynamic measurement

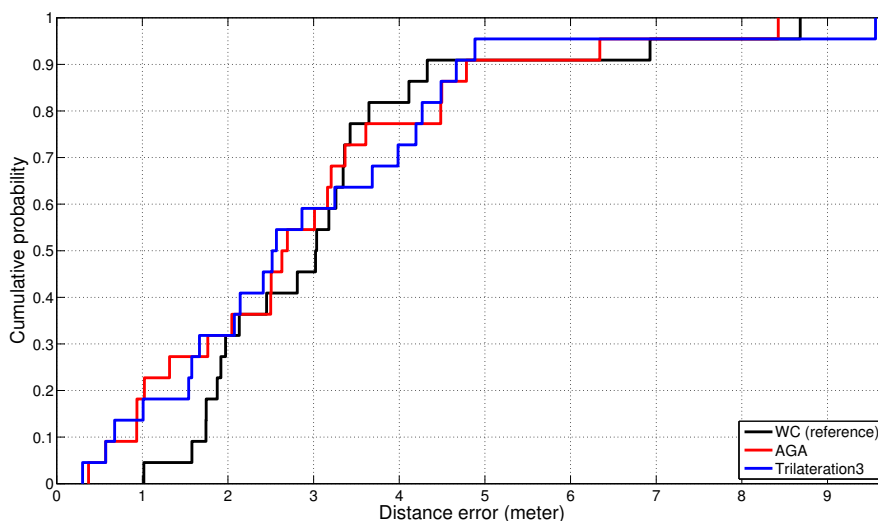


As we did in the previous analysis, we begin with the average localization errors shown in Figure 5.10. Again the two best performing algorithms are AGA and Trilateration as before. The smallest localization error is achieved by AGA with approximately 2.91 meters accuracy. The Trilateration reaches an accuracy of about 2.94 meters in average. LLS and TrilatN on the other hand are not able to accomplish an average localization error below our reference value of circa 3.16 meters. Thus, LLS achieves a accuracy of 3.32 meters and the TrilatN algorithm, which does have even more issues, attains an error of almost 3.8 meters. Due to the bad performance of LLS as well as TrilatN, we do not evaluate them any further.

In Figure 5.11 CDF of the localization errors for AGA and Trilateration are shown. Compared to the analysis from the static measurement, both algorithms are very similar. The smallest localization error of Trilat begins at 0.37 meter and AGA just starts at 0.3 meter. Except the maximal error, both versions of WAILA grow generally steady. The largest localization error of AGA amounts 8.42 meters, whereas Trilat measures up to 9.5 meters.

When we compare the performance of the Weighted Centroid with both versions of WAILA, our algorithm improves the localization again. Even though the enhancement is smaller compared to the static measurement, WAILA improves the localization accuracy by approximately

**Figure 5.11:** CDF of the localization errors by WAILA in the dynamic measurement



0.25 meter. Again both versions achieve a smaller minimal error than the reference performance. This time one of the algorithms, the Adaptive Geometric Algorithm, also accomplishes a smaller maximal localization error.

As can be seen in Figure 5.11, the gap between WC and AGA/Trilat curves from Figure 5.6 can be found again. Both algorithms improve at least the smallest 30% of all localization errors. Between the 30% and 40% marks, Trilat partly enhances the errors, whereas AGA is only able to keep up with the performance of WC. After the 40% mark, both algorithms again improve the localization errors up to the 60% mark. For the remaining errors, both algorithms mainly achieve a slightly less good performance. However, AGA as well as the Trilateration versions of WAILA are once again able to improve the localization accuracy compared to WC. Despite the rather difficult environment, our algorithm achieves better results than the very stable Weighted Centroid algorithm.

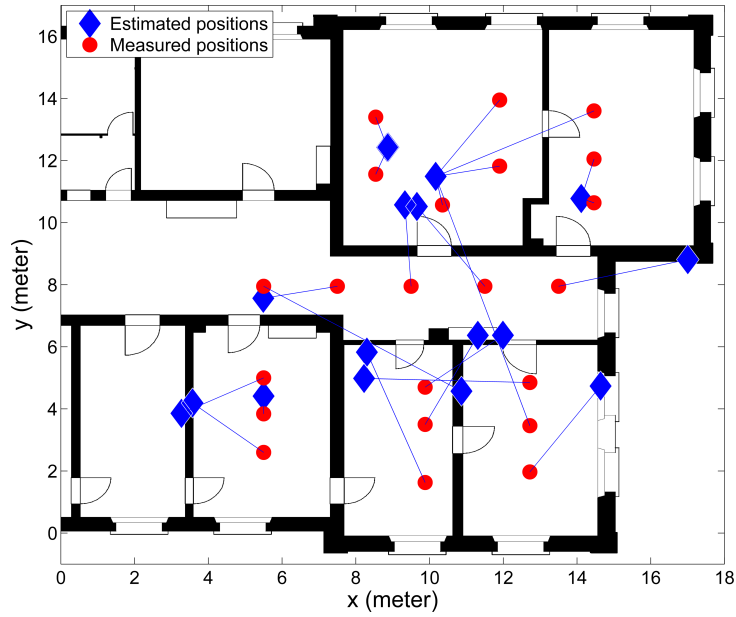
Figure 5.12 shows the localization errors when using the WAILA with Adaptive Geometric Algorithm. Once again, the localized positions seem to be more random and less structured as compared to the ones located by WC. However, the locations are better distributed and not all pulled towards the anchor nodes. When comparing based on the room-level, both algorithms archive with almost 60% the same accuracy.

It is noticeable that multiple measurements are located onto the same positions. This is not caused by an error in the computations, but a special case, which cannot be solved by AGA. Due to the dynamic measurement, people that stand in LOS to an anchor node lead to an incorrect distance assumption. If this estimated distance is very large compared to the distances of the other anchor nodes, the AGA algorithm is not able to find an intersection between all circles.

Finding no intersection of the circles is a common issue for all the geometric algorithm. Therefore, to address this issue, we simply select the weighted centre<sup>3</sup> between the anchor nodes.

<sup>3</sup>weighted by the radii (=distances)

**Figure 5.12:** Localized positions by WAILA (w/ AGA) in the dynamic measurement



However, this workaround then leads to these artefacts, where multiple localizations are mapped onto the same position.

Despite this problematic location of AGA, the localization accuracy could be once more improved compared to WC.



## Chapter 6

---

# Conclusions

### 6.1 Summary & Conclusions

Even today indoor localization is a hard to solve issue. In this thesis, we constructed our own indoor localization algorithm, which we call WAILA in Chapter 3. The general idea is to use an adapted path loss model, so that we can transform any measured RSS into a distance measure. In order to achieve this goal, we selected an improved model that bases on the Log-Normal Path Loss model. Such model, the Wall Attenuation Factor Path Loss model, additionally includes the signal attenuation caused by walls. Hence, we could improve the range estimations based on wall approximations that we did. With the help of further algorithms, e.g. the threshold algorithm, more improvements in the range estimation could be achieved. Finally, we proposed to use different localization algorithms to establish a final position from the range measures.

For the preliminary experimental analysis in Chapter 4, we performed multiple measurements. From its data, we could determine essential environment based information as for example the path loss values, WAF and threshold boundaries. Thanks to new insights and knowledge gained from this experimental analysis, we could then finally start with the evaluation.

Therefore, in Chapter 5 we evaluated the performance of WAILA under two different conditions. First during the weekend, representing a static environment without any people or moving obstacles in our examined area. Second, while the working hours with people in their offices or wandering around, which were causing an ever changing and dynamic environment in terms of the signal distribution. The evaluation showed that no matter what environment we tested in, our algorithm could improve the localization accuracy. Therefore, we compared the performance with the results achieved by the Weighted Centroid, a stable and well performing range-free approach. From the four proposed localization methods used in WAILA, we selected the Adaptive Geometric Algorithm as well as the Trilateration as the best performing ones.

### 6.2 Future Work

Depending on the deployment of the anchor nodes, the localization accuracy may vary. Therefore, further research could determine best practices for the deployment of the anchor nodes. A connection between the amount of anchor nodes used and the localization error could be

analysed. Additionally the compatibility between different setups in the environment and localization algorithms could reveal good as well as bad patterns for the deployment of the anchor nodes.

When using different algorithms in the proximity step of WAILA, closer position estimations might be achieved. Hence further algorithms could be discovered and improve the overall result of our created algorithm.

# Appendices



## Appendix A

---

# Site Survey

**Table A.1:** Anchor nodes

ID	$x$	$y$
1	8.2	15.6
2	16.6	9.8
3	10.7	1.4
4	3.8	2.3

**Table A.2:** Measurements

ID	$x$	$y$	AN <sub>1</sub> mean(RSS)	AN <sub>2</sub> mean(RSS)	AN <sub>3</sub> mean(RSS)	AN <sub>4</sub> mean(RSS)
1	15.8	9.9	-34.955	-9.238	-53.027	-59.351
2	15.8	11.5	-45.857	-24.396	-58.409	-66.863
3	15.8	13.3	-36.800	-31.933	-51.877	-54.881
4	15.8	15.1	-33.543	-33.812	-49.997	-65.307
5	13.9	15.1	-28.608	-32.887	-60.929	-61.761
6	13.9	13.4	-31.530	-34.647	-51.321	-64.986
7	13.9	11.6	-33.691	-34.872	-48.121	-66.094
8	13.9	9.9	-40.131	-15.860	-55.208	-53.260
9	11.9	15.4	-31.838	-47.473	-50.066	-56.966
10	11.9	13.5	-25.771	-30.999	-43.165	-58.423
11	11.9	11.8	-43.346	-15.854	-42.891	-53.973
12	11.9	10.1	-32.730	-24.979	-41.140	-56.874
13	10.5	10.1	-28.961	-34.094	-39.612	-48.108
14	10.5	11.9	-24.703	-38.148	-44.586	-48.254
15	10.5	13.4	-29.329	-34.732	-42.728	-53.740
16	10.5	15.1	-31.417	-37.025	-48.361	-59.442
17	8.4	15.1	-20.214	-41.233	-35.091	-59.024

**Table A.2:** Measurements

ID	$x$	$y$	AN <sub>1</sub> mean(RSS)	AN <sub>2</sub> mean(RSS)	AN <sub>3</sub> mean(RSS)	AN <sub>4</sub> mean(RSS)
18	8.4	13.6	-32.620	-35.304	-49.866	-62.997
19	8.4	11.8	-39.629	-38.018	-34.817	-51.747
20	8.4	9.9	-28.800	-33.013	-37.869	-57.639
21	13.8	5.4	-47.507	-52.720	-45.491	-49.209
22	13.8	3.8	-46.162	-48.405	-43.770	-41.466
23	13.8	2.3	-45.164	-53.572	-49.236	-44.533
24	13.8	0.8	-42.658	-52.815	-42.148	-42.317
25	12.1	0.8	-47.873	-45.594	-31.271	-48.031
26	12.1	2.3	-49.539	-44.888	-29.909	-42.651
27	12.1	3.8	-54.857	-46.678	-30.553	-43.789
28	12.1	5.3	-45.972	-44.129	-42.589	-45.179
29	10.3	0.8	-41.928	-56.735	-21.432	-31.470
30	10.3	2.3	-42.742	-61.571	-19.112	-65.122
31	10.3	3.8	-37.523	-56.137	-28.153	-33.298
32	10.3	5.3	-34.387	-48.164	-30.324	-33.431
33	8.4	5.3	-40.156	-54.128	-45.334	-40.864
34	8.4	3.8	-40.270	-56.431	-23.256	-36.321
35	8.4	2.3	-53.791	-55.533	-16.414	-40.487
36	8.4	0.8	-49.074	-63.558	-21.628	-50.238
37	6.3	5.9	-57.258	-55.570	-42.891	-30.151
38	6.3	4.4	-61.112	-52.990	-34.285	-21.416
39	6.3	2.9	-53.878	-54.441	-23.063	-15.323
40	6.3	1.5	-53.400	-62.186	-29.810	-13.742
41	4.3	1.5	-56.253	-65.947	-22.593	-12.699
42	4.3	2.9	-54.926	-57.105	-29.008	-15.858
43	4.3	4.4	-46.231	-62.543	-39.399	-20.549
44	4.3	5.9	-54.614	-47.496	-31.698	-24.965
45	14	8.0	-39.308	-31.745	-48.606	-47.708
46	12.5	8.0	-37.344	-38.667	-41.036	-45.809
47	11	8.0	-42.531	-54.275	-46.239	-48.152
48	9.5	8.0	-35.623	-36.044	-29.233	-38.427
49	8	8.0	-45.611	-40.480	-31.096	-36.391
50	6.5	8.0	-35.852	-43.909	-41.523	-39.094

## Appendix B

# Corridor Path Loss Model

**Table B.1:** Linear regression

$x_i$ $\log_{10}(d)$	$y_i$ RSS	$x_i - \bar{x}$	$y_i - \bar{y}$	$\frac{(x_i - \bar{x})}{(y_i - \bar{y})}$	$(x_i - \bar{x})^2$	$(y_i - \bar{y})^2$	$\hat{y}$
-0.3	-3.544	-0.991	15.400	-15.267	0.983	237.169	-1.803
0	-4.350	-0.690	14.594	-10.075	0.477	212.984	-7.008
0.2	-11.411	-0.514	7.533	-3.874	0.264	56.745	-10.052
0.3	-11.212	-0.389	7.733	-3.010	0.152	59.791	-12.213
0.4	-14.687	-0.292	4.257	-1.245	0.086	18.120	-13.888
0.5	-13.961	-0.213	4.984	-1.063	0.046	24.836	-15.258
0.5	-20.880	-0.146	-1.936	0.283	0.021	3.749	-16.415
0.6	-9.393	-0.088	9.551	-0.843	0.008	91.216	-17.418
0.7	-19.803	-0.037	-0.859	0.032	0.001	0.738	-18.302
0.7	-16.379	0.009	2.565	0.022	0.000	6.578	-19.093
0.7	-19.873	0.050	-0.929	-0.047	0.003	0.863	-19.809
0.8	-17.754	0.088	1.190	0.105	0.008	1.416	-20.463
0.8	-23.793	0.123	-4.849	-0.594	0.015	23.516	-21.064
0.8	-20.423	0.155	-1.479	-0.229	0.024	2.186	-21.620
0.9	-23.289	0.185	-4.345	-0.803	0.034	18.882	-22.138
0.9	-28.260	0.213	-9.316	-1.982	0.045	86.780	-22.623
0.9	-32.552	0.239	-13.608	-3.254	0.057	185.185	-23.078
1.0	-20.698	0.264	-1.753	-0.463	0.070	3.074	-23.507
1.0	-23.828	0.287	-4.884	-1.404	0.083	23.856	-23.913
1.0	-25.524	0.310	-6.579	-2.037	0.096	43.288	-24.299
1.0	-27.613	0.331	-8.669	-2.868	0.110	75.150	-24.665
1.0	-23.268	0.351	-4.324	-1.518	0.123	18.696	-25.014
1.1	-22.289	0.370	-3.345	-1.239	0.137	11.191	-25.348
1.1	-19.873	0.389	-0.929	-0.361	0.151	0.863	-25.668

$$b = \frac{\sum (x_i - \bar{x})(y_i - \bar{y})}{\sum (x_i - \bar{x})^2} = \frac{-51.7327}{2.9919} = -17.2908 \quad (\text{B.1})$$

$$a = \bar{y} - b \cdot \bar{x} = -18.9441 - (-17.2908 \cdot 0.6903) = -7.0077 \quad (\text{B.2})$$

$$r^2 = \left( \frac{\sum ((x_i - \bar{x}) \cdot (y_i - \bar{y}))}{\sqrt{\sum (x_i - \bar{x})^2 \cdot \sum (y_i - \bar{y})^2}} \right)^2 = \left( \frac{-51.7327}{\sqrt{2.9919 \cdot 1206.9}} \right)^2 = 0.7412 \quad (\text{B.3})$$

$$(\text{B.4})$$

As result of the linear regression, we receive the following linear formula:

$$y = a + b \cdot x \quad (\text{B.5})$$

$$y = -7.0077 + -17.2908 \cdot x, \quad (\text{B.6})$$

$$(\text{B.7})$$

where  $x = \log(\text{distance})$ .

## Appendix C

---

### Static Measurement

**Table C.1:** Anchor nodes

ID	$x$	$y$
1	8.4	15.5
2	15.8	15.9
3	14.5	0.6
4	3.6	2.0

**Table C.2:** Measurements

ID	$x$	$y$	AN <sub>1</sub> mean(RSS)	AN <sub>2</sub> mean(RSS)	AN <sub>3</sub> mean(RSS)	AN <sub>4</sub> mean(RSS)
1	14.5	13.6	-41.559	-24.396	-51.529	-59.097
2	14.5	12.1	-46.040	-32.213	-58.980	-57.725
3	14.5	10.6	-36.831	-26.255	-42.815	-59.572
4	12.7	4.9	-38.790	-48.636	-23.568	-52.770
5	12.7	3.5	-44.693	-49.050	-23.162	-46.830
6	12.7	2.0	-43.149	-45.307	-24.416	-53.014
7	9.9	1.6	-40.428	-61.557	-33.077	-48.581
8	9.9	3.5	-41.090	-51.559	-39.967	-55.810
9	9.9	4.7	-45.676	-48.751	-33.175	-46.024
10	5.5	5	-58.118	-64.741	-43.313	-23.457
11	5.5	3.8	-49.505	-59.967	-44.584	-16.452
12	5.5	2.6	-54.923	-61.078	-51.401	-9.923
13	8.5	13.4	-15.089	-35.830	-54.156	-61.518
14	8.5	11.6	-24.408	-48.731	-56.070	-48.805
15	10.4	10.6	-26.430	-34.352	-37.164	-45.299
16	11.9	11.8	-36.269	-33.728	-58.634	-50.977
17	11.9	14.0	-36.751	-29.214	-55.980	-54.887

**Table C.2:** Measurements

ID	$x$	$y$	AN <sub>1</sub> mean(RSS)	AN <sub>2</sub> mean(RSS)	AN <sub>3</sub> mean(RSS)	AN <sub>4</sub> mean(RSS)
18	13.5	8.0	-46.590	-38.544	-45.635	-50.250
19	11.5	8.0	-27.957	-42.166	-33.664	-47.879
20	9.5	8.0	-25.560	-42.299	-42.496	-43.847
21	7.5	8.0	-50.726	-51.036	-40.466	-38.455
22	5.5	8.0	-62.525	-46.487	-52.587	-25.377

## Appendix D

---

# Dynamic Measurement

**Table D.1:** Anchor nodes

ID	$x$	$y$
1	8.4	15.5
2	15.8	15.9
3	14.5	0.6
4	3.6	2.0

**Table D.2:** Measurements

ID	$x$	$y$	AN <sub>1</sub> mean(RSS)	AN <sub>2</sub> mean(RSS)	AN <sub>3</sub> mean(RSS)	AN <sub>4</sub> mean(RSS)
1	14.5	13.6	-38.061	-39.416	-53.169	-53.692
2	14.5	12.1	-43.460	-27.954	-48.961	-56.864
3	14.5	10.6	-47.541	-32.995	-50.715	-53.585
4	12.7	4.9	-39.802	-42.977	-27.585	-54.568
5	12.7	3.5	-37.175	-42.701	-44.413	-54.038
6	12.7	2.0	-47.273	-40.453	-15.561	-47.253
7	9.9	1.6	-40.950	-54.415	-31.129	-31.926
8	9.9	3.5	-37.763	-51.053	-36.510	-41.681
9	9.9	4.7	-35.780	-56.534	-27.997	-39.625
10	5.5	5	-56.116	-60.256	-43.526	-21.200
11	5.5	3.8	-51.743	-59.572	-48.502	-15.770
12	5.5	2.6	-55.945	-63.934	-52.594	-15.155
13	8.5	13.4	-16.285	-39.337	-53.828	-53.572
14	8.5	11.6	-16.318	-44.357	-46.934	-53.455
15	10.4	10.6	-30.564	-39.512	-46.257	-51.861
16	11.9	11.8	-33.510	-42.529	-53.825	-52.092
17	11.9	14.0	-30.118	-37.129	-50.347	-51.291

**Table D.2:** Measurements

ID	$x$	$y$	AN <sub>1</sub> mean(RSS)	AN <sub>2</sub> mean(RSS)	AN <sub>3</sub> mean(RSS)	AN <sub>4</sub> mean(RSS)
18	13.5	8.0	-40.127	-30.296	-32.999	-48.301
19	11.5	8.0	-24.514	-40.374	-46.516	-49.533
20	9.5	8.0	-35.910	-40.644	-44.070	-49.224
21	7.5	8.0	-40.472	-58.740	-52.637	-29.802
22	5.5	8.0	-39.801	-45.918	-54.228	-26.610

## Appendix E

---

### Localization Errors

**Table E.1:** Localization errors of the static measurement (in meters)

ID	WC	LLS	TrilatN	Trilateration	AGA
1	1.865	2.966	2.088	0.540	1.789
2	3.065	3.667	3.528	1.009	1.318
3	3.844	1.719	3.363	2.306	1.098
4	2.333	5.207	3.156	4.931	6.302
5	1.982	1.589	1.223	2.031	1.801
6	1.350	4.939	4.546	1.501	2.751
7	3.742	2.455	1.374	5.912	5.262
8	4.852	6.019	3.375	3.997	3.914
9	2.768	2.782	2.515	2.241	1.532
10	3.148	3.748	3.230	2.877	1.707
11	2.333	0.092	1.279	1.139	1.067
12	1.968	4.613	5.757	1.698	2.384
13	2.074	3.449	2.620	0.042	0.614
14	3.301	1.457	1.957	0.816	1.328
15	2.250	2.573	3.296	2.766	2.067
16	2.903	4.185	4.186	2.660	1.861
17	2.095	1.007	0.438	3.510	3.869
18	3.363	2.252	0.278	3.175	4.561
19	3.062	0.235	0.989	0.570	3.062
20	5.503	4.782	5.228	1.932	2.057
21	4.279	4.333	3.860	4.448	3.402
22	5.242	6.377	6.263	7.521	3.972
AVG	3.060	3.010	2.930	2.610	2.620

**Table E.2:** Localization errors of the dynamic measurement (in meters)

ID	WC	LLS	TrilatN	Trilateration	AGA
1	3.022	2.389	3.311	4.666	4.784
2	2.809	3.630	3.528	1.009	1.318
3	3.426	3.187	4.583	0.676	0.372
4	1.018	4.128	3.404	4.195	4.496
5	8.681	11.037	9.013	9.561	8.425
6	1.743	3.026	5.251	4.883	3.367
7	1.745	5.170	3.651	3.986	4.484
8	3.360	2.108	1.074	3.685	3.205
9	1.875	2.743	2.088	2.515	2.693
10	3.178	2.238	3.350	2.864	2.504
11	2.451	2.114	2.371	0.573	0.573
12	1.917	5.867	6.726	1.541	2.499
13	1.971	1.760	2.682	0.303	1.024
14	3.646	4.265	2.607	1.667	0.934
15	3.260	3.783	2.079	2.075	0.937
16	3.035	1.715	0.756	2.142	1.765
17	1.579	2.037	2.054	2.412	3.010
18	2.132	3.445	3.243	1.577	3.609
19	6.928	5.887	6.058	4.267	3.162
20	4.327	4.496	5.277	3.248	2.629
21	4.113	4.730	4.686	2.566	2.045
22	3.344	3.954	5.720	4.488	6.342
AVG	3.162	3.320	3.790	2.940	2.910

# List of Abbreviations

**AGA** Adaptive Geometric Algorithm.

**AN** anchor node.

**CDF** Cumulative Distribution Function.

**GPS** Global Positioning System.

**LLS** Linear Least Square.

**LNPL** Log-Normal Path Loss.

**LOS** line of sight.

**MN** mobile node.

**NLS** Non-Linear Least Square.

**NN** Nearest Neighbour.

**NRN** Nearest Room Neighbour.

**RSS** Received Signal Strength.

**TDOA** Time Difference of Arrival.

**TM** Threshold Matrix.

**TOA** Time of Arrival.

**Trilat** Trilateration.

**TrilatN** Trilateration with  $n$  anchor nodes.

**USRPN** Universal Software Radio Peripheral.

**WAF** Wall Attenuation Factor.

**WAFPL** Wall Attenuation Factor Path Loss.

**WAILA** Wall Attenuation Indoor Localization Algorithm.

**WC** Weighted Centroid.

## Bibliography

- [1] Sarkar, Tapan K., et al. "A survey of various propagation models for mobile communication." *Antennas and Propagation Magazine, IEEE* 45.3 (2003): 51-82.
- [2] Gonçalo, Gomes, and Sarmento Helena. "A novel approach to indoor location systems using propagation models in wsns." *International Journal on Advances in Networks and Services* 2.4 (2010): 251-260.
- [3] Bahl, Paramvir, and Venkata N. Padmanabhan. "RADAR: An in-building RF-based user location and tracking system." *INFOCOM 2000. Nineteenth Annual Joint Conference of the IEEE Computer and Communications Societies. Proceedings. IEEE. Vol. 2. Ieee, 2000.*
- [4] Lotker, Zvi, Marc Martinez De Albeniz, and Stéphane Pérénnes. "Range-free ranking in sensors networks and its applications to localization." *Ad-Hoc, Mobile, and Wireless Networks. Springer Berlin Heidelberg, 2004. 158-171.*
- [5] He, Tian, et al. "Range-free localization and its impact on large scale sensor networks." *ACM Transactions on Embedded Computing Systems (TECS)* 4.4 (2005): 877-906..
- [6] Blumenthal, Jan, et al. "Weighted centroid localization in zigbee-based sensor networks." *Intelligent Signal Processing, 2007. WISP 2007. IEEE International Symposium on. IEEE, 2007.*
- [7] He, Tian, et al. "Range-free localization schemes for large scale sensor networks." *Proceedings of the 9th annual international conference on Mobile computing and networking. ACM, 2003.*
- [8] Yang, Jie, and Yingying Chen. "Indoor localization using improved rss-based lateration methods." *Global Telecommunications Conference, 2009. GLOBECOM 2009. IEEE. IEEE, 2009.*
- [9] Gezici, Sinan, Ismail Guvenc, and Zafer Sahinoglu. "On the performance of linear least-squares estimation in wireless positioning systems." *Communications, 2008. ICC'08. IEEE International Conference on. IEEE, 2008.*
- [10] Brida, Peter, and Juraj Machaj. "A Novel Enhanced Positioning Trilateration Algorithm Implemented for Medical Implant In-Body Localization." *International Journal of Antennas and Propagation* 2013 (2013).

- [11] Kim, Bumgon, Wonsun Bong, and Yong C. Kim. "Indoor localization for Wi-Fi devices by cross-monitoring AP and weighted triangulation." Consumer Communications and Networking Conference (CCNC), 2011 IEEE. IEEE, 2011.
- [12] Fet, Ngewi, Marcus Handte, and Pedro José Marrón. "A model for WLAN signal attenuation of the human body." Proceedings of the 2013 ACM international joint conference on Pervasive and ubiquitous computing. ACM, 2013.
- [13] Bensky, Alan. Wireless positioning technologies and applications. Artech House, 2007.
- [14] Bshara, Mussa, et al. "Fingerprinting localization in wireless networks based on received-signal-strength measurements: A case study on WiMAX networks." Vehicular Technology, IEEE Transactions on 59.1 (2010): 283-294.
- [15] Koweerawong, Chavalit, Komwut Wipusitwarakun, and Kamol Kaemarungsi. "Indoor localization improvement via adaptive RSS fingerprinting database." Information Networking (ICOIN), 2013 International Conference on. IEEE, 2013.
- [16] Zhong, Zigu. Range-free localization and tracking in wireless sensor networks. Diss. University of Minnesota, 2010.
- [17] Hirsbrunner Simon. "Indoor Localisation In Wi-Fi-Networks Using An Improved Centroid Approach." University of Berne, Communication and Distributed Systems, Bachelor Thesis, 2014.